BUCKLING OF THIN ANNULAR PLATES DUE TO RADIAL COMPRESSIVE LOADING

Thesis by

Saurindranath Majumdar

In Partial Fulfillment of the Requirements

For the Degree of

Aeronautical Engineer

California Institute of Technology

Pasadena, California

1968

ACKNOWLEDGMENT

The author wishes to express his sincere appreciation to (1) Dr. Ernest E. Sechler, who suggested the experiments, for his help and encouragement, (2) Dr. C. D. Babcock for his advice and comments, (3) M. Jessey, C. Hemphill and R. Luntz for their help in setting up the experiments, (4) Mrs. Betty wood for her excellent drawings and Mrs. Elizabeth Fox for bearing with my handwriting and typing the manuscript so skillfully.

ABSTRACT

Buckling of circular annular plates with the outer edge clamped and the inner edge free loaded with a uniform radial compressive force applied at the outside edge has been studied both theoretically and experimentally. A differential equation of equilibrium of the buckled plate has been developed for any general deflection pattern and solutions corresponding to the buckled form $w_n(r)\ \mathrm{Cos}\, n\theta$ have been sought. The differential equation has been solved exactly for $n = 0$ and $n = 1$ and approximately for higher values of n as well as for $n = 0$ and 1. The solutions indicate that, for small ratios of inner to outer radius, the plates buckle into a radially symmetric buckling mode, but for the ratio of inner to outer radius exceeding a certain minimum value the minimum buckling load corresponds to buckling modes with waves along the circumference, the number of which depends on the particular ratio of the inner and outer radii. Tests were carried out using thin aluminium plates and the results agreed reasonably well with the theoretical predictions.

TABLE OF CONTENTS

LIST OF SYMBOLS

a	=	Outer radius
b	=	Inner radius
h	=	Thickness of plate
N_o	=	Radial compressive force at the outer edge
$N_{o_{cr}}$	=	Critical radial compressive force at the outer edge
E	=	Modulus of elasticity of aluminium
E_s	=	Modulus of elasticity of steel
D	=	Stiffness of plate = $\frac{Eh^3}{12(1-\nu^2)}$
ν	=	Poisson's ratio, assumed equal to 1/3
N_r	=	Radial stress resultant
N_θ	=	Circumferential stress resultant
$N_{r\theta}$	=	Shear stress resultant
e_r, e_θ	=	In-plane radial and circumferential strain prior to buckling
e'_r, e'_θ	=	In-plane strain during buckling
U	=	Strain energy
V	=	Potential energy
u, v	=	In-plane radial and circumferential displacement perturbations
w	=	Transverse displacement perturbation
T	=	Temperature rise above ambient
θ_c	=	Theoretical buckling temperature
T_c	=	Experimentally observed buckling temperature
α_s, α_A	=	Coefficients of thermal expansion of steel and aluminium

INTRODUCTION

It is well known (1)* that (assuming a radially symmetric buckling mode) the radial buckling load $N_{o_{cr}}$ of a circular plate with a hole at the center can be expressed as

$$N_{o_{cr}} = k \frac{D}{a^2} \tag{1}$$

where k is a numerical factor, the magnitude of which depends on the b/a ratio. The value of k for various b/a ratios for a clamped outside edge and free inner edge is shown in figure 1. It is seen that k reaches a minimum for b/a = 0.2 and for ratios larger than 0.2, k increases rapidly without bound. This may be explained by noting that for b/a approaching unity, the compressed ring with the outer boundary clamped behaves like a long compressed rectangular plate clamped along a long side and free along the other. Such a plate will buckle into many waves. Thus it could reasonably be expected that in the case of a narrow ring, several waves will be formed along the circumference and the values of k obtained by assuming a symmetric buckling mode will have higher values.

The stability of a thin annular plate under uniform compressive forces applied at both edges was treated by Olsson (4) and Schubert (5) for several boundary conditions, but in these investigations, the deflection surface was assumed to be radially symmetric. Yamaki (2) took into account the possibility of waves in the circumferential direction of the buckled plate, but his calculations showed that for the case

---

* Numbers in parentheses indicate reference numbers at the end.

with the outer edge clamped and the inner edge free, the minimum buckling load still corresponded to a radially symmetric buckling mode.

The purpose of this report was to study the buckling mode of a circular isotropic plate with a concentric hole loaded radially at the outer edge which was clamped and having the edge of the hole free. The effect of the b/a ratio on the buckling load was sought and the possibility of antisymmetric modes of buckling was investigated. A short series of simple tests were carried out to check the validity of the theory.

THEORY

Assumptions

(i) The usual Kirchhoff's hypothesis regarding the variation of displacement and stresses through the thickness of the plate are made.

(ii) The displacement perturbations are assumed to be small so that the in-plane Lamé stresses prior to buckling do not undergo any appreciable amount of change during buckling.

(iii) The system is assumed to be perfect.

Derivation of Governing Equation

The in-plane equation of equilibrium is

$$\frac{N_\theta - N_r}{r} - \frac{dN_r}{dr} = 0 \tag{2}$$

The Lamé solution for the plane stress case is

$$N_r = -N_o \frac{a^2}{a^2-b^2}\left(1 - \frac{b^2}{r^2}\right) \tag{3a}$$

$$N_\theta = -N_o \frac{a^2}{a^2-b^2}\left(1 + \frac{b^2}{r^2}\right) \tag{3b}$$

$$N_{r\theta} = 0 \tag{3c}$$

The strains prior to buckling are

$$e_r = \frac{1}{hE}(N_r - \nu N_\theta) \tag{4a}$$

$$e_\theta = \frac{1}{hE}(N_\theta - \nu N_r) \tag{4b}$$

The strain energy due to contraction of the midplane before buckling is given by

$$U_1 = \frac{1}{2hE} \int_o^{2\pi} \int_b^a (N_r^2 + N_\theta^2 - 2\nu N_r N_\theta) r d\theta dr \tag{5}$$

During buckling, the in-plane stresses do further work and the in-plane strains after bending may be written as

$$e'_r = \frac{\partial u}{\partial r} + \frac{1}{2}\left(\frac{\partial w}{\partial r}\right)^2 \tag{6a}$$

$$e'_\theta = \frac{u}{r} + \frac{1}{r}\frac{\partial v}{\partial \theta} + \frac{1}{2r^2}\left(\frac{\partial w}{\partial \theta}\right)^2 \tag{6b}$$

Assuming that the forces N_r, N_θ remain constant during bending, the strain energy due to additional contraction of the middle plane is

$$U_2 = \int_b^a \int_o^{2\pi} [N_r e'_r + N_\theta e'_\theta] \, r d\theta dr \tag{7}$$

$$= \int_b^a \int_o^{2\pi} \left[N_r \frac{\partial u}{\partial r} + N_\theta \frac{u}{r} + \frac{N_\theta}{r}\frac{\partial v}{\partial \theta}\right] r d\theta dr +$$

$$\int_b^a \int_o^{2\pi} \frac{1}{2}\left[N_r \left(\frac{\partial w}{\partial r}\right)^2 + \frac{N_\theta}{r^2}\left(\frac{\partial w}{\partial \theta}\right)^2\right] r d\theta dr$$

The strain energy due to bending is

$$U_B = \frac{D}{2} \int_b^a \int_o^{2\pi} \left\{ \left(\frac{\partial^2 w}{\partial r^2} + \frac{1}{r}\frac{\partial w}{\partial r} + \frac{1}{r^2}\frac{\partial^2 w}{\partial \theta^2} \right)^2 - 2(1-\nu)\frac{\partial^2 w}{\partial r^2}\left(\frac{1}{r}\frac{\partial w}{\partial r} + \frac{1}{r^2}\frac{\partial^2 w}{\partial \theta^2}\right) \right.$$

$$\left. + 2(1-\nu)\left(\frac{1}{r}\frac{\partial^2 w}{\partial r \partial \theta} - \frac{1}{r^2}\frac{\partial w}{\partial \theta}\right)^2 \right\} r d\theta dr \tag{8}$$

Therefore, the total strain energy of the plate is

$$\overline{U} = U_B + U_1 + U_2$$

The first integral of eq. (7) can be written with the help of eq. (2) as

$$\int_b^a \int_o^{2\pi} \left\{ N_r \frac{\partial u}{\partial r} + u\left(\frac{N_r}{r} + \frac{dN_r}{dr}\right) + \frac{N_\theta}{r} \frac{\partial v}{\partial \theta} \right\} r d\theta dr$$

$$= \int_b^a \int_o^{2\pi} \left\{ \frac{\partial}{\partial r}(urN_r) + N_\theta \frac{\partial v}{\partial \theta} \right\} d\theta dr$$

$$= \int_o^{2\pi} urN_r \Big|_{r=b}^{r=a} d\theta + \int_b^a N_\theta v \Big|_{\theta=0}^{\theta=2\pi} dr - \int_b^a \int_o^{2\pi} \frac{\partial N_\theta}{\partial \theta} v d\theta dr$$

Since $\frac{\partial N_\theta}{\partial \theta} = 0$, by using the boundary conditions, the above becomes

$$= \int_o^{2\pi} uaN_r(a) d\theta$$

which is equal to the work done by the external force. Thus

$$U_2 = W + U'$$

where W = work done by external force

U' = work produced by the in-plane stresses due to bending.

∴ Total potential energy of the system, V, is given by

$$V = \overline{U} - U_1 - W.$$

$$= \frac{1}{2} \int_b^a \int_o^{2\pi} \left\{ N_r \left(\frac{dw}{\partial r}\right)^2 + \frac{N_\theta}{r^2} \left(\frac{\partial w}{\partial \theta}\right)^2 + D\left[\left(\frac{\partial^2 w}{\partial r^2} + \frac{1}{r}\frac{\partial w}{\partial r} + \frac{1}{r^2}\frac{\partial^2 w}{\partial \theta^2}\right)^2 - \right.\right.$$

$$\left.\left. -2(1-\nu)\frac{\partial^2 w}{\partial r^2}\left(\frac{1}{r}\frac{\partial w}{\partial r} + \frac{1}{r^2}\frac{\partial^2 w}{\partial \theta^2}\right) + 2(1-\nu)\left(\frac{1}{r}\frac{\partial^2 w}{\partial r \partial \theta} - \frac{1}{r^2}\frac{\partial w}{\partial \theta}\right)^2 \right] \right\} r d\theta dr \qquad (9)$$

The differential equation of equilibrium may be obtained from eq. (9) by making the potential energy of the system have a stationary value

$$\delta V = 0 \qquad (10)$$

The variation of the first two terms give

$$\delta\int_b^a\int_o^{2\pi}\left[\frac{N_r}{2}\left(\frac{\partial w}{\partial r}\right)^2+\frac{N_\theta}{2r^2}\left(\frac{\partial w}{\partial\theta}\right)^2\right]r\,d\theta dr$$

$$=\int_b^a\int_o^{2\pi}\left(rN_r\frac{\partial^2 w}{\partial r^2}+N_\theta\frac{\partial w}{\partial r}+\frac{N_\theta}{r}\frac{\partial^2 w}{\partial\theta^2}\right)\delta w\,d\theta dr$$

$$+\int_o^{2\pi}rN_r\frac{\partial w}{\partial r}\,\delta w\Bigg|_{r=b}^{r=a}d\theta+\int_b^a\frac{N_\theta}{r}\frac{\partial w}{\partial\theta}\,\delta w\Bigg|_o^{2\pi}dr$$

$$=\int_b^a\int_o^{2\pi}\left(rN_r\frac{\partial^2 w}{\partial r^2}+N_\theta\frac{\partial w}{\partial r}+\frac{N_\theta}{r}\frac{\partial^2 w}{\partial\theta^2}\right)\delta w\,d\theta dr$$

The variation of the rest of the term gives

$$\delta\frac{D}{2}\int_b^a\int_o^{2\pi}\left[\left(\frac{\partial^2 w}{\partial r^2}+\frac{1}{r}\frac{\partial w}{\partial r}+\frac{1}{r^2}\frac{\partial^2 w}{\partial\theta^2}\right)^2-2(1-\nu)\frac{\partial^2 w}{\partial r^2}\left(\frac{1}{r}\frac{\partial w}{\partial r}+\frac{1}{r^2}\frac{\partial^2 w}{\partial\theta^2}\right)\right.$$
$$\left.+2(1-\nu)\left(\frac{1}{r}\frac{\partial^2 w}{\partial r\partial\theta}-\frac{1}{r^2}\frac{\partial w}{\partial\theta}\right)^2\right]r\,d\theta dr$$

$$=D\int_b^a\int_o^{2\pi}\left\{r\frac{\partial^4 w}{\partial r^4}+2\frac{\partial^3 w}{\partial r^3}-\frac{1}{r}\frac{\partial^2 w}{\partial r^2}+\frac{1}{r^2}\frac{\partial w}{\partial r}+\frac{1}{r^3}\frac{\partial^4 w}{\partial\theta^4}+\frac{2}{r^3}\frac{\partial^2 w}{\partial\theta^2}+\frac{2\nu}{r}\frac{\partial^4 w}{\partial r^2 d\theta^2}-\right.$$
$$\left.\frac{2\nu}{r^2}\frac{\partial^3 w}{\partial r\partial\theta^2}+\frac{2\nu}{r^3}\frac{\partial^2 w}{\partial\theta^2}+2(1-\nu)\left(\frac{1}{r}\frac{\partial^4 w}{\partial r^2\partial\theta^2}-\frac{1}{r^2}\frac{\partial^3 w}{\partial r\partial\theta^2}+\frac{1}{r^3}\frac{\partial^2 w}{\partial\theta^2}\right)\right\}\delta w\,dr\,d\theta$$
$$+D\left[\int_o^{2\pi}\left[\left\{r\frac{\partial^2 w}{\partial r^2}\frac{\partial\delta w}{\partial r}\Bigg|_b^a-\frac{\partial}{\partial r}\left(r\frac{\partial^2 w}{\partial r^2}\right)\delta w\Bigg|_b^a+\frac{1}{r}\frac{\partial w}{\partial r}\,\delta w\Bigg|_b^a\right\}+\left\{\frac{1}{r^2}\frac{\partial^2 w}{\partial\theta^2}\,\delta w\Bigg|_b^a\right.\right.\right.$$
$$\left.+\nu\frac{\partial w}{\partial r}\frac{\partial\delta w}{\partial r}\Bigg|_b^a+\frac{\nu}{r}\frac{\partial^2 w}{\partial\theta^2}\frac{\partial\delta w}{\partial r}\Bigg|_b^a+\frac{\nu}{r^2}\frac{\partial^2 w}{\partial\theta^2}\delta w-\frac{\nu}{r}\frac{\partial^3 w}{\partial r\partial\theta^2}\,\delta w\Bigg|_b^a\right\}$$
$$\left.\left.+2(1-\nu)\left\{-\frac{1}{r}\frac{\partial^3 w}{\partial r\partial\theta^2}\,\delta w\Bigg|_b^a+\frac{1}{r^2}\frac{\partial^2 w}{\partial\theta^2}\,\delta w\Bigg|_b^a\right\}\right]d\theta\right]$$

Adding all the variations, we get the Euler equation as

$$rD\nabla^4 w - rN_r \frac{\partial^2 w}{\partial r^2} - N_\theta \left(\frac{\partial w}{\partial r} + \frac{1}{r}\frac{\partial^2 w}{\partial \theta^2}\right) = 0 \tag{11}$$

and the boundary conditions

$$\int_0^{2\pi} D\left(r\frac{\partial^2 w}{\partial r^2} + \nu\frac{\partial w}{\partial r} + \frac{\nu}{r}\frac{\partial^2 w}{\partial \theta^2}\right)\frac{\partial \delta w}{\partial r}\Bigg|_b^a d\theta = 0$$

$$\int_0^{2\pi} D\left(\frac{1}{r}\frac{\partial w}{\partial r} - \frac{\partial^2 w}{\partial r^2} - r\frac{\partial^3 w}{\partial r^3} + \frac{1}{r^2}\frac{\partial^2 w}{\partial \theta^2} + \frac{\nu}{r^2}\frac{\partial^2 w}{\partial \theta^2} - \frac{-2(1-\nu)}{r}\frac{\partial^3 w}{\partial r \partial \theta^2} - \right.$$

$$\left.\frac{\nu}{r}\frac{\partial^3 w}{\partial r \partial \theta^2} + \frac{2(1-\nu)}{r^2}\frac{\partial^2 w}{\partial \theta^2}\right)\delta w\Bigg|_b^a d\theta = 0$$

Since in the present case the outer edge is clamped and the inner edge free

$$rD\left[\frac{\partial^2 w}{\partial r^2} + \nu\left(\frac{1}{r}\frac{\partial w}{\partial r} + \frac{1}{r^2}\frac{\partial^2 w}{\partial \theta^2}\right)\right] = 0 \quad \text{at } r = b \tag{12}$$

and

$$rD\left[-\frac{\partial}{\partial r}\left(\frac{\partial^2 w}{\partial r^2} + \frac{1}{r}\frac{\partial w}{\partial r} + \frac{1}{r^2}\frac{\partial^2 w}{\partial \theta^2}\right) - \frac{1-\nu}{r}\frac{\partial}{\partial \theta}\left(\frac{1}{r}\frac{d^2 w}{\partial r \partial \theta} - \frac{1}{r^2}\frac{\partial w}{\partial \theta}\right)\right] = 0$$

at $r = b$

or $$r\left[Q_r - \frac{1}{r}\frac{\partial M_{r\theta}}{\partial \theta}\right] = 0 \qquad \text{at } r = b \tag{13}$$

We also have

$$\frac{\partial w}{\partial r} = 0 \quad \text{at } r = a \tag{14}$$

$$w = 0 \quad \text{at } r = a \tag{15}$$

Substituting for N_r and N_θ from eq. (3) into eq. (11) and defining

$$\lambda = \frac{N_o b^2 a^2}{D(a^2-b^2)} \tag{16}$$

we get

$$\nabla^4 w + \lambda\left(\frac{1}{b^2} + \frac{1}{r^2}\right)\nabla^2 w = \frac{2\lambda}{r^2}\frac{\partial^2 w}{\partial r^2} \tag{17}$$

Try $w = A_n \cos n\theta$ as a solution.

Substituting this into (17) and cancelling $\cos n\theta$ we get

$$\frac{d^4A_n}{dr^4} + \frac{2}{r}\frac{d^3A_n}{dr^3} - \left\{\frac{1+2n^2+\lambda}{r^2} - \frac{\lambda}{b^2}\right\}\frac{d^2A_n}{dr^2} + \left\{\frac{1+2n^2+\lambda}{r^3} + \frac{\lambda}{rb^2}\right\}\frac{dA_n}{dr}$$

$$+ \left\{\frac{n^2(n^2-\lambda-4)}{r^4} - \frac{\lambda n^2}{b^2r^2}\right\} A_n = 0 \tag{18}$$

Making a substitution of $z = \sqrt{\lambda}\,\frac{r}{b}$ gives

$$\frac{d^4A_n}{dz^4} + \frac{2}{z}\frac{d^3A_n}{dz^3} - \left\{\frac{1+2n^2+\lambda}{z^2} - 1\right\}\frac{d^2A_n}{dz^2} + \left\{\frac{1+2n^2+\lambda}{z^3} + \frac{1}{z}\right\}\frac{dA_n}{dz}$$

$$+ \left\{\frac{n^2(n^2-\lambda-4)}{z^4} - \frac{n^2}{z^2}\right\} A_n = 0 \tag{19}$$

Eq. (19) together with the boundary conditions (12)-(15) properly transformed poses an eigenvalue problem. When $n = 0$, the result is radially symmetric buckling and eq. (19) reduces to

$$\frac{d^3\psi}{dz^3} + \frac{2}{z}\frac{d^2\psi}{dz^2} + \left(1 - \frac{1+\lambda}{z^2}\right)\frac{d\psi}{dz} + \left(\frac{1+\lambda}{z^3} + \frac{1}{z}\right)\psi = 0 \tag{20}$$

where $\psi = \frac{dA_n}{dz}$.

A solution of eq. (20) satisfying boundary condition (13) is

$$\psi = A J_p(z) + B J_{-p}(z) \tag{21}$$

$$p = \sqrt{\lambda+1}$$

The imposition of boundary conditions (12) and (14), properly transformed, yield the following equation

$$\begin{vmatrix} J_p(\sqrt{\lambda}\,\frac{a}{b}) & J_{-p}(\sqrt{\lambda}\,\frac{a}{b}) \\ J_{p-1}(\sqrt{\lambda}) + \frac{\nu-p}{\sqrt{\lambda}}\,J_p(\sqrt{\lambda}) & J_{-p}(\sqrt{\lambda})\,(\frac{\nu+p}{\sqrt{\lambda}}) + J_{-1-p}(\sqrt{\lambda}) \end{vmatrix} = 0$$

A plot of the result obtained is given in Timoshenko's "Theory of Elastic Stability" and is reproduced here on fig. 2.

n = 1

Eq. (19) reduces to

$$\frac{d^4A_n}{dz^4} + \frac{2}{z}\,\frac{d^3A_n}{dz^3} + (1 - \frac{3+\lambda}{z^2})\,\frac{d^2A_n}{dz^2} + \left\{\frac{3+\lambda}{z^3} + \frac{1}{z}\right\}\frac{dA_n}{dz}$$

$$-\left\{\frac{\lambda+3}{z^4} + \frac{1}{z^2}\right\}A_n = 0 \qquad (22)$$

Substituting

$$A_n = \phi z \quad \text{and} \quad \frac{d\phi}{dz} = \psi \qquad (23)$$

this reduces to

$$\frac{d^3\psi}{dz^3} + \frac{6}{z}\,\frac{d^2\psi}{dz^2} + (\frac{3-\lambda}{z^2} + 1)\,\frac{d\psi}{dz} + (\frac{3}{z} - \frac{\lambda+3}{z^3})\,\psi = 0 \qquad (24)$$

This could further be reduced to

$$\frac{d^2\psi}{dz^2} + \frac{3}{z}\,\frac{d\psi}{dz} + \left[1 + \frac{1-p^2}{z^2}\right]\psi = \frac{C}{z^3} \qquad (25)$$

where c is an arbitrary constant and

$$\lambda = p^2 - 4$$

The general solution of eq. (25) is

$$\psi = \frac{1}{z}\left[A\,J_p(z) + B\,J_{-p}(z) + CS_{-1,p}(z)\right] \tag{26}$$

where

$$S_{-1,p} = \frac{\pi}{2\mathrm{Sin}p\pi}\left[J_p(z)\int \frac{J_{-p}(z)}{z}\,dz - J_{-p}(z)\int \frac{J_p(z)}{z}\,dz\right] \tag{27}$$

and is called the Lommel function. With the help of eq. (23), eq. (26) can be written as

$$z\frac{dA_n}{dz} - A_n = z\left[A\,J_p(z) + B\,J_{-p}(z) + CS_{-1,p}(z)\right] \tag{28}$$

The boundary conditions (12)-(15) reduce to

$$A_n = \frac{dA_n}{dz} = 0 \quad \text{at} \quad z = \sqrt{\lambda}\,a/b \tag{29a}$$

$$\frac{d^2A_n}{dz^2} + \frac{\nu}{z^2}\left\{z\frac{dA_n}{dz} - A_n\right\} = 0 \quad \text{at } z = \sqrt{\lambda} \tag{29b}$$

$$\frac{d^3A_n}{dz^3} + \frac{1}{z^2}\frac{d^2A_n}{dz^2} - \frac{3-\nu}{z^2}\frac{dA_n}{dz} + \frac{3-\nu}{z^3}A_n = 0 \quad \text{at } z = \sqrt{\lambda} \tag{29c}$$

Satisfying these boundary conditions leads to the following equations

$$A\,J_p\left(\sqrt{\lambda}\,\frac{a}{b}\right) + B\,J_{-p}\left(\sqrt{\lambda}\,\frac{a}{b}\right) = 0$$

$$A\left\{(1+\nu-p)\,J_p(\sqrt{\lambda}) + \sqrt{\lambda}\,J_{p-1}(\sqrt{\lambda})\right\} + B\left\{(1+\nu+p)\,J_{-p}(\sqrt{\lambda}) + \sqrt{\lambda}\,J_{-p-1}(\sqrt{\lambda})\right\} = 0$$

$$C = 0$$

For a nontrivial solution of A and B, we must have

$$\begin{vmatrix} (1+\nu-p)J_p(\sqrt{\lambda}) + \sqrt{\lambda}\, J_{p-1}(\sqrt{\lambda}) & (1+\nu+p)J_{-p}(\sqrt{\lambda}) + \sqrt{\lambda}\, J_{-p-1}(\sqrt{\lambda}) \\ J_p(\sqrt{\lambda}\,\frac{a}{b}) & J_{-p}(\sqrt{\lambda}\,\frac{a}{b}) \end{vmatrix} = 0$$

A plot of the result is given on fig. 2.

Approximate Solution (Energy Method)

Assume a deflection pattern

$$w = A_n(r)\,\mathrm{Cos}\, n\theta$$

Putting this expression in eq. (9) and integrating over θ, we get

$$V = \frac{\pi}{2}\int_b^a \left\{ N_r A_n'^2 + \frac{N_\theta}{r^2} n^2 A_n^2 + D\left[\left(A_n'' + \frac{1}{r}A_n' - \frac{n^2 A_n}{r^2}\right)^2 - 2(1-\nu)A_n''\left(\frac{1}{r}A_n' - \frac{n^2 A_n}{r^2}\right) + 2(1-\nu)\left(\frac{nA_n}{r^2} - \frac{nA_n'}{r}\right)^2\right]\right\} r\,d\theta\,dr$$

for $n \neq 0$ (30)

and

$$V = \pi\int_b^a \left\{ N_r A_n'^2 + D\left[(A_n'' + \frac{1}{r}A_n')^2 - 2(1-\nu)\frac{A_n''}{r}A_n'\right]\right\} r\,d\theta\,dr$$

for $n = 0$ (31)

where $(\,)'$ denotes differentiation with respect to r.

For the purpose of calculation the function A_n was chosen to be

$$A_n(r) = w_o\left(1 - \frac{r^2}{a^2}\right)^2$$

It satisfied all the displacement boundary conditions. From fig. 2 it is seen that the difference between the exact and the approximate

solutions for n = 0 and n = 1 is not too large, especially for large b/a ratio. Hence, in carrying out the approximate solutions for n greater than 1, the same form for A_n was chosen.

Putting this value of A_n in eqs. (30) and (31) and substituting for N_r and N_θ from eq. (3) and minimising V with respect to w_o, we get

$$\lambda_{cr} = \frac{(\frac{n^4}{2} + \frac{2}{3}n^2)\frac{a^2}{b^2} + (\frac{5}{3}n^4 - \frac{44}{3}n^2 + \frac{32}{3}) + (-3n^4 + 20n^2 - \frac{64}{3})\frac{b^2}{a^2} + (n^4 - \frac{20}{3}n^2 + \frac{128}{3})\frac{b^4}{a^4} - (\frac{n^4}{6} - \frac{2}{3}n^2 + 32)\frac{b^6}{a^6} - 4n^2(n^2-4)\log\frac{a}{b}}{(\frac{2}{3} - \frac{13}{24}n^2)\frac{a^2}{b^2} + (\frac{11}{3}n^2 - \frac{8}{3}) - (\frac{9}{2}n^2 - 4)\frac{b^2}{a^2} + (\frac{5}{3}n^2 - \frac{8}{3})\frac{b^4}{a^4} - (\frac{7}{24}n^2 - \frac{2}{3})\frac{b^6}{a^6} + n^2(\frac{a^2}{b^2} - 4)\log\frac{a}{b}}$$

for $n \neq 0$

and

$$\lambda_{cr} = \frac{\frac{2}{3} - \frac{4}{3}(\frac{b}{a})^2 + \frac{8}{3}(\frac{b}{a})^4 - 2(\frac{b}{a})^6}{\frac{1}{24}(\frac{a}{b})^2 - \frac{1}{6} + \frac{1}{4}(\frac{b}{a})^2 - \frac{1}{6}(\frac{b}{a})^4 + \frac{1}{24}(\frac{b}{a})^6}$$

for $n = 0$

From eq. (16)

$$\lambda = \frac{N_o b^2 a^2}{D(a^2 - b^2)}$$

$$\therefore \quad N_{o_{cr}} = \lambda_{cr}\frac{D}{a^2}(\frac{a^2}{b^2} - 1) = k\frac{D}{a^2}$$

where $k = \lambda_{cr}(\frac{a^2}{b^2} - 1)$

The value of k as a function of b/a has been plotted for n = 0, 1, 2, 3, 4, 5, 6 and 10 on fig. 3. The exact solutions for n = 0 and n = 1 are plotted with the approximate ones in fig. 2 and it is seen that they agree reasonably well for high b/a ratio. It is evident from fig. 3 that the trajectory of the minimum buckling load increases with b/a ratio without bound. This could be explained by the following analogy. It is known that a long rectangular plate with one of its long edges fixed and the other free has a buckling load given by

$$N_{x_{cr}} = \frac{k'D}{d^2}$$

where d is the width of the plate and k' is a constant.

In the case of a circular plate when b/a approaches unity, the compressed ring behaves like a plate, as described above. Therefore, if we redefine a constant k' such that

$$N_{\theta_{cr}}(a) = \frac{k'D}{(a-b)^2}$$

then k' should approach a finite limit as b/a approaches unity.

$$k' = \lambda_{cr} \frac{\left\{1 + \frac{b^2}{a^2}\right\}\left(1 - \frac{b}{a}\right)^2}{\frac{b^2}{a^2}} = k \frac{\left(1 + \frac{b^2}{a^2}\right)\left(1 - \frac{b}{a}\right)}{1 + \frac{b}{a}}$$

A plot of k' against b/a shown in fig. 4 indicates that the k' corresponding to minimum buckling load remains finite as b/a approaches unity. The value of k' for an infinitely long rectangular plate is shown in fig. 4.

TEST RESULTS

To check the validity of the theory, some simple tests were carried out using 0.041'' thick aluminium plates clamped between two 0.5'' thick steel rings by means of 12– 1/2''ϕ high tensile steel bolts as shown in fig. 5. The inner diameter of the steel rings was 8'' and the outer diameter 10''. The following sized holes were used in the plates:

b	b/a
0''	0
0.5''	0.125
2''	0.5
2.5''	0.625

The loading was accomplished by heating the whole assembly, so that due to different coefficients of expansions, the steel rings put a uniformly distributed radial compressive load on the plate. The effect of the elasticity of the rings on the stress distribution in the plates and on the assumption of clamped edge condition is discussed in Appendix A. The tests were done in two parts.

Test Series A

The assembly was placed inside a Missimers environment chamber in which the temperature could be held at any value for any length of time. Strain gauges were attached to the two faces of the plate and a pair of opposing gauges R_1 and R_2 were connected to two legs of a Wheatstone bridge as shown in fig. 7. The reading of the voltmeter, amplified by a factor of 10, was directly proportional to the difference between the strains experienced by R_1 and R_2 and

gave a measure of the bending of the plate as shown in Appendix B.

Strain gauges were connected both in the circumferential and in the radial direction for the plates with b = 0'', 0.5 and 2'', and only in the circumferential direction for the plate with b = 2.5''. SR4 Baldwin gauges were used for the plates with b = 0'' and b = 0.5'' and temperature compensated micromeasurement foil gauges were used for the plates with larger holes. Copper-Constantine thermocouples were soldered onto a brass washer and several of these brass washers were attached to the plate as well as to the steel rings. After each increment of temperature, the assembly was allowed to soak heat for about 45 minutes to one hour, or until the temperature indicated by the different thermocouples were the same. This temperature was checked with the reading of a thermometer placed inside the chamber. The maximum error in measuring the temperature was $\pm 1^{\circ}F$. Derivation of the critical temperature θ_c at which buckling occurs is given in Appendix A.

Tests were carried out to measure the difference in the coefficients of expansion of aluminium and steel. A value of 6.6×10^{-6} per $^{\circ}F$ was used for $(\alpha_A - \alpha_S)$ for the purpose of calculations.

Due to the presence of initial imperfections the plates started to bend from the beginning of loading and a Southwell type plot was used to determine the buckling temperature T_c of the perfect plates. The reliability of the Southwell plot has been proven for a solid plate in Appendix B. In plotting the Southwell plot, points near the origin have been ignored since for small T the percentage error in measuring T is large; also points corresponding to temperatures that

are comparable with θ_c have been ignored, since the Southwell plot does not hold for such large values of T. See Figs. 8-15 inc.

Test Series B

An attempt was made to measure the number of waves along the circumference of the plates during buckling by means of an inductance pickup. The plate clamped by the rings was placed on a turn table; the pickup was attached by means of an arm to a graduated optical bench and could be raised or lowered by means of a turning knob as shown in fig. 16. The assembly was heated by means of a 1000 watt quartz iodine photographic lamp. The general test setup is shown in fig. 17. The lamp was connected in series with a rheostat so that the current through it could be controlled. The pickup was fixed at a given height from the plate and the current through the lamp was increased in steps. At every step, sufficient time was allowed to let the assembly reach an equilibrium state and then the plate was rotated by turning the turn table and the output of the pickup was plotted directly on an X-Y plotter. Fig. 18 gives the calibration curve for the pickup and the effect of temperature on it. It is seen that the effect of temperature on the calibration curve is small and for the purpose of measuring the number of waves around the circumference it was adequate. It was assumed that, though the temperature distribution in the plate was nonuniform, it would only deform the shapes of the waves around the circumference and would not change the number. The test results from the different sized plates are given on figures 19 to 23. A thermocouple attached to the plate gave an average value of the temperature of the plate.

DISCUSSION OF EXPERIMENTAL RESULTS

The theoretical buckling temperature θ_c for each case has been indicated together with the experimentally observed buckling temperature T_c in fig. 8 to fig. 15. The values of k computed from the experimentally observed buckling temperature have been plotted in fig. 3. The difference between the theoretical and the experimentally observed values of k are of the order of 10%. This discrepancy is mainly due to the inaccuracy in measuring the temperature and also due to the slight temperature variation in the plate and the steel rings which could not be avoided. Another possible source of error lay in the fact that, though the voltage output from the strain gauges was amplified 10 times, its magnitude was very small and thus small error in measuring the voltage resulted in considerable relative error. A direct displacement measurement of the plates under loading would be more desirable, but setting up displacement measuring devices inside the furnace was inconvenient because of lack of space as well as giving temperature problems. By using two strain gauges on the two faces of the plates as two legs of a Wheatstone bridge, the effect of temperature on the voltage output was minimised because both strain gauges were heated to almost the same temperature and any effect of temperature on the resistance of the strain gauges was balanced out.

In test series B, the calibration curve for voltage vs. distance varied slightly with temperature and so the distance given on figs. 19 to 23 are not very accurate. But, since the purpose of the tests was to measure the number of waves around the circumference only, the

effect of temperature on the calibration curve did not affect the results. The plots in figs. 19 and 20 for b/a = 0 and 0.125 show the buckle pattern to be radially symmetric, as expected. In fig. 21, for the case of b/a = 0.5 the buckling mode is seen to be radially symmetric, i.e., n = 0. According to the approximate analysis, whose results are shown in fig. 3, the buckling mode should be n = 1 though the curve corresponding to n = 0 lies closely above it. In fig. 2 where the exact solutions are drawn, the curves for n = 0 and n = 1 intersect at b/a = 0.5. The fact that the experimental result showed n = 0 could be explained by observing that the plate had more initial imperfection in the n = 0 mode than in the n = 1 mode, which agrees with the physical intuition that imperfections with longer wavelengths are more probable than with shorter wavelengths and that axisymmetric imperfections are most predominant. For the case with b/a = 0.625 (fig. 22) the plate first starts to deflect in the n = 0 mode, but with rise of temperature it goes into the n = 2 mode. According to fig. 3, the curves for n = 2 and n = 3 almost intersect at b/a = .625. For the case with b/a = 0.75 (fig. 23), the plate first starts deflecting in the axisymmetric mode, but with rise of temperature goes into the n = 5 mode, which agrees with the theoretical wave number given in the figure. These tests conclusively prove that, for clamped outside edge and free inner edge, the plate buckles with waves along the circumference for b/a exceeding a certain minimum value close to 0.5.

CONCLUSION

(1) The energy method using just one term gives a reasonable approximation to the true buckling load, particularly for large b/a ratios.

(2) For small values of b/a ratio the radially symmetric mode gives the lowest buckling load. As b/a is increased, an unsymmetric mode with waves in the circumferential direction gives a lower buckling load than the symmetric mode and the number of waves increases with an increasing b/a ratio.

(3) The theoretical buckling load increases beyond bound as b/a approaches unity, but it must be remembered that as b/a approaches unity, the thickness h becomes of the same order of magnitude as (a-b), and hence the theory which is based on the assumption that h is very small compared to the other dimensions of the plate is no longer valid.

(4) It would be interesting to measure the initial imperfection of the plate and do a Fourier analysis on it and experimentally measure how the coefficient of each component grows with the load.

(5) For large b/a ratios, the buckling curves for different n's are crowded together. Thus for any given b/a ratio in this range, the plate will probably start to buckle in that mode in which the maximum initial imperfection is present. To check whether the plate bifurcates into another mode at higher load, a full nonlinear analysis has to be carried out.

REFERENCES

1. Timoshenko, S.: Theory of Elastic Stability, McGraw Hill, New York (1936).
2. Yamaki, N.: "Buckling of a Thin Annular Plate Under Uniform Compression", Journal of Applied Mechanics, A.S.M.E., Vol. 25, p. 267 (1958).
3. Timoshenko, S.: Strength of Materials, Part II, D. Van Nostrand Company, Inc., New York (1930).
4. Olsson, R. Gran: "Über axialsymmetrische knickung dünner Kreisringplatten", Ingenieur-Archiv, Bd. 8 (1937), S.449.
5. Schubert, A.: "Die Beullast dünner Kreisringplatten, die am Aussen- und Innenrand gleichmässigen Druck erfahren", Zeitschrift für angewandte Mathematik und Mechanik, Bd 25/27.
6. Dean, W. R.: "The Elastic Stability of an Annular Plate", Proceedings of the Royal Society of London, England, Series A, Vol. 106 (1924), p. 268.
7. Meissner, E.: "Über das knicken kreisringförmiger Scheiben", Scheweizerche Bauzeitung, Bd. 101 (1933), s. 87.
8. Timoshenko, S.: "Theory of Plates and Shells", McGraw-Hill Book Company, Inc., New York and London, 1960.
9. Luke, Y. L.: Integrals of Bessel Functions, McGraw Hill Book Company, Inc.
10. Jahnke-Emde: Tables of Functions, Verlag und Druck von B. G. Teubner in Leipzig and Berlin.

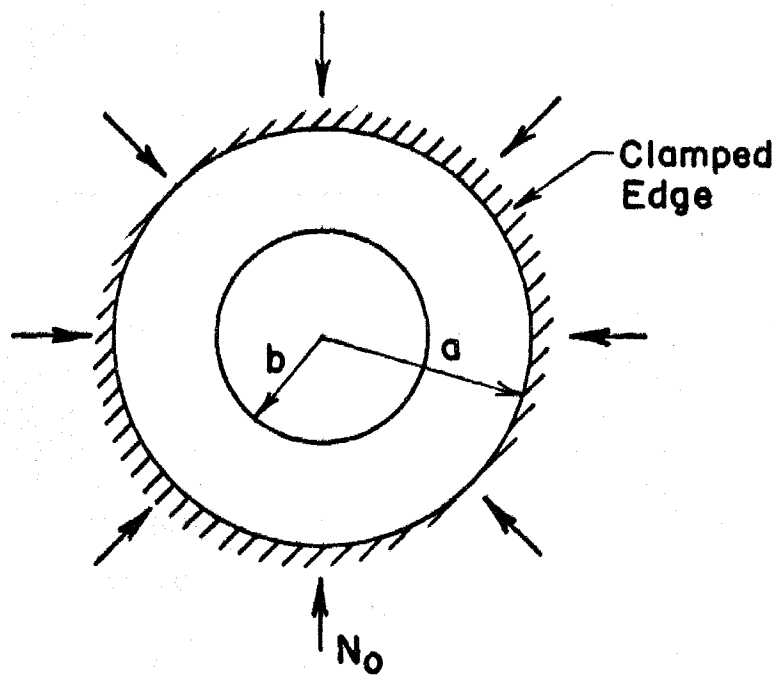

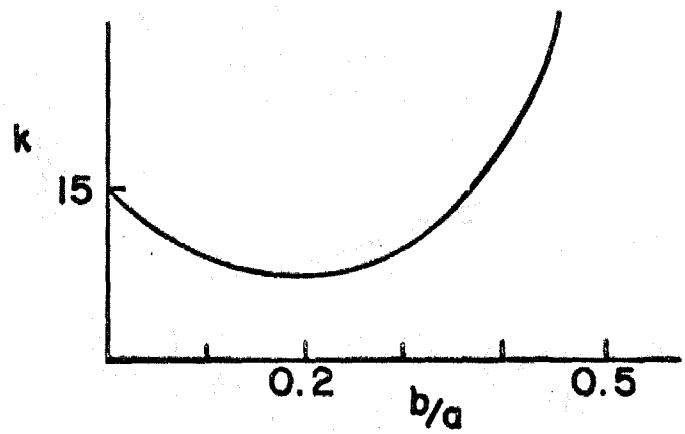

FIG. 1

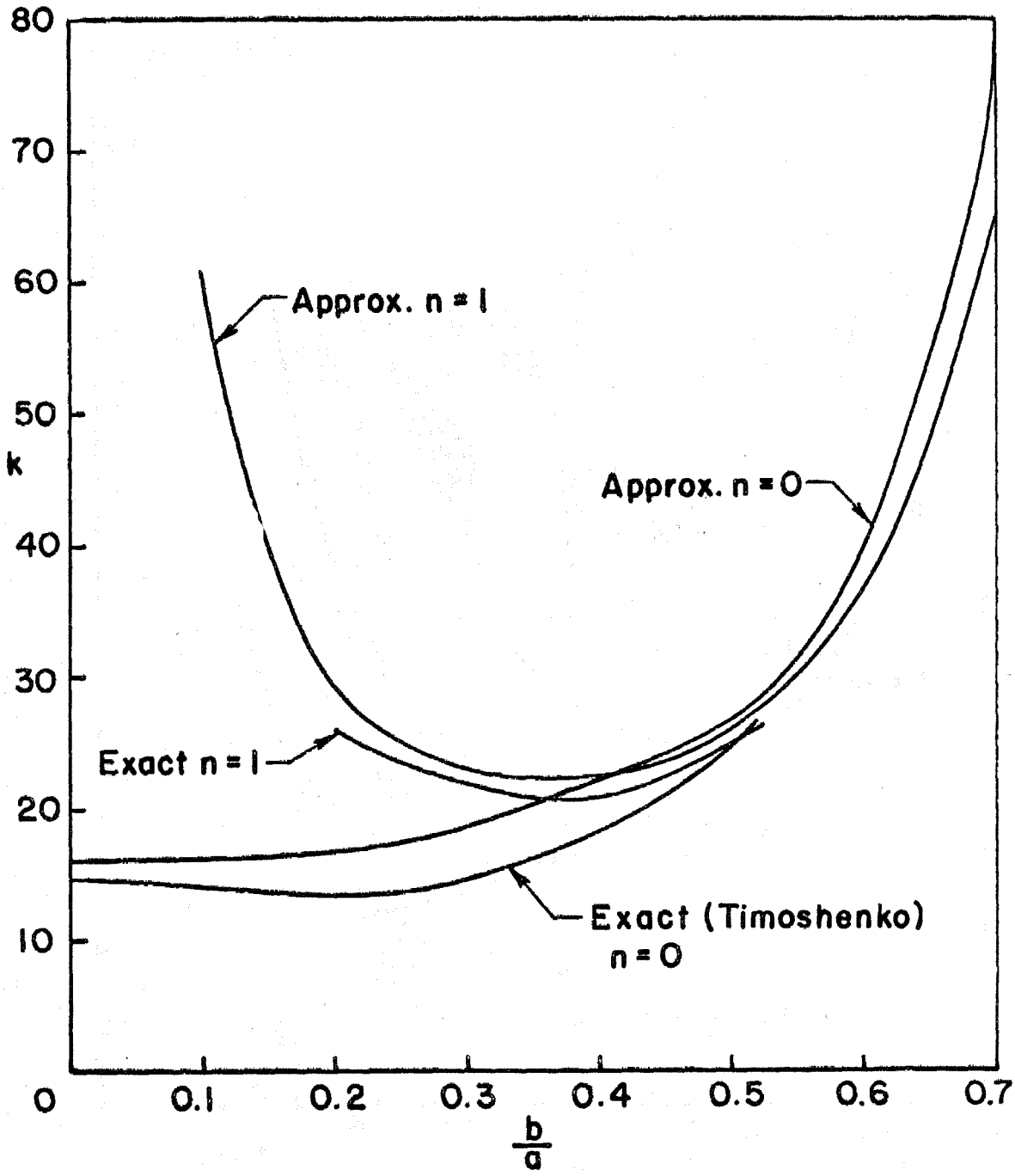
80
70
60
50
k
40
30
20
10
0
0.1
0.2
0.3
0.4
0.5
0.6
0.7
b/a
Approx. n = 1
Approx. n = 0
Exact n = 1
Exact (Timoshenko)
n = 0

FIG. 2

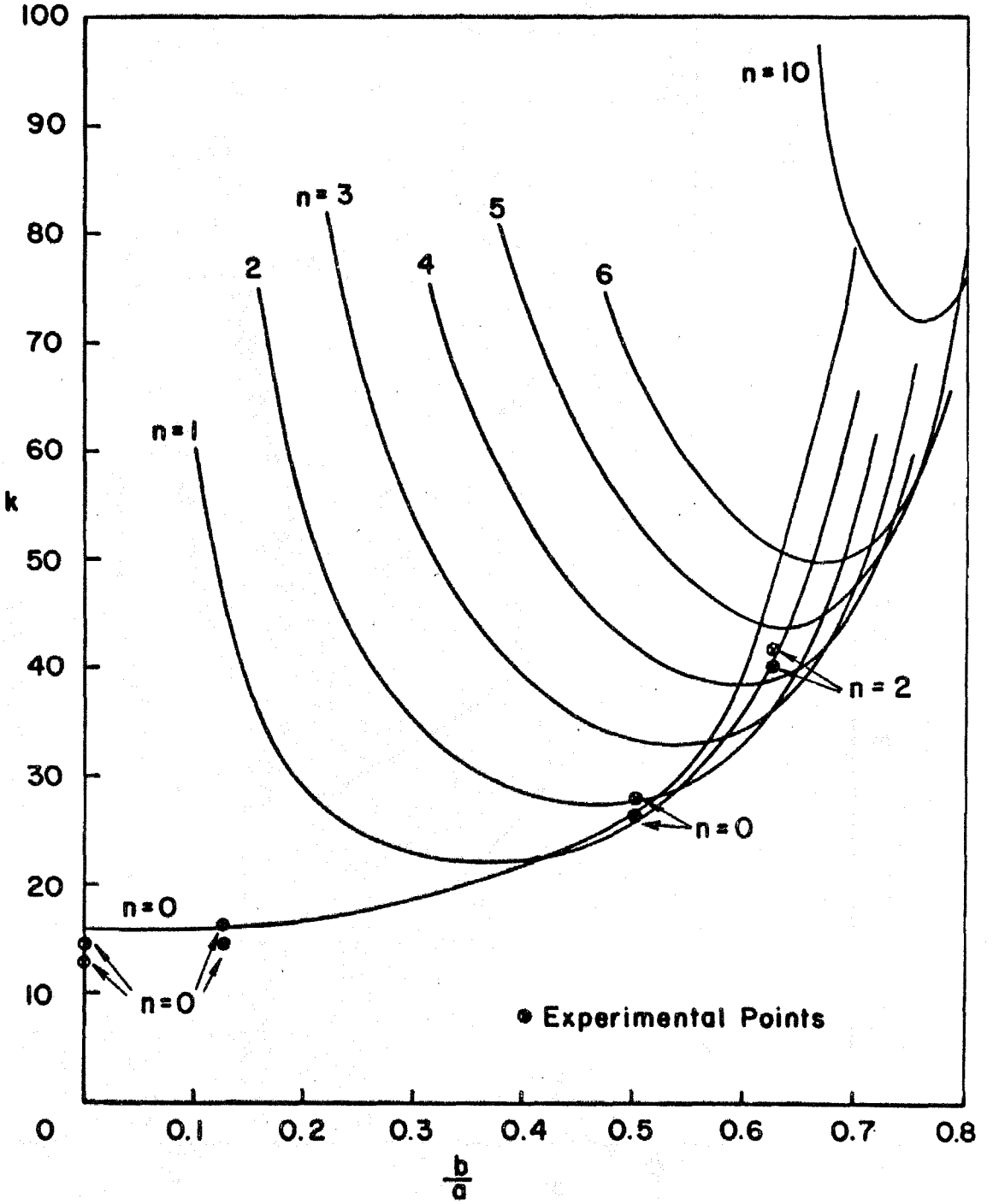
100
90
80
70
60
50
40
30
20
10
0
k
0.1
0.2
0.3
0.4
0.5
0.6
0.7
0.8
b/a
n=10
n=3
5
4
2
6
n=1
n=2
n=0
n=0
n=0
Experimental Points

FIG. 3

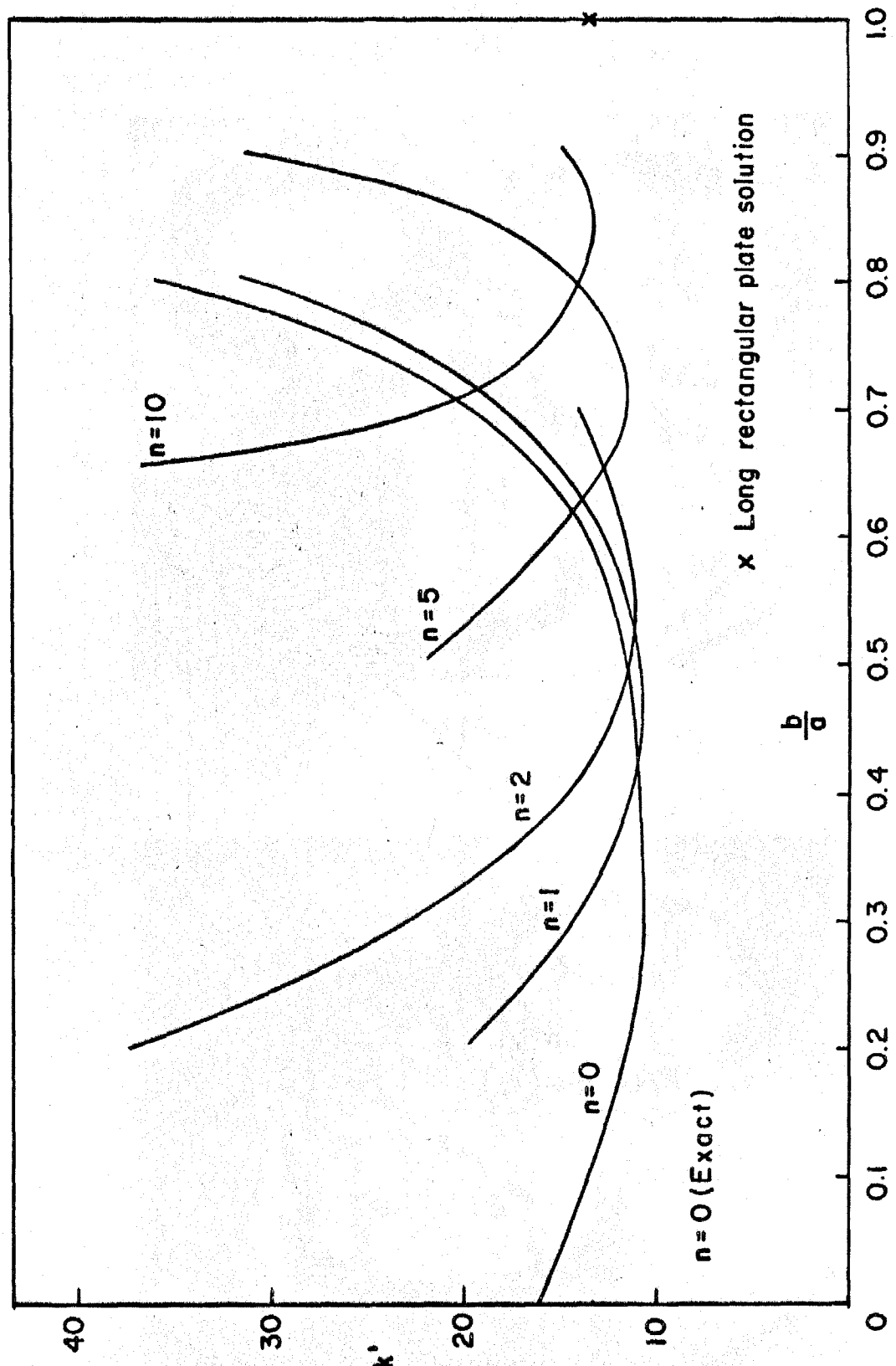
k'
40
30
20
10
0
0.1
0.2
0.3
0.4
0.5
0.6
0.7
0.8
0.9
1.0
b/a
n=10
n=5
n=2
n=1
n=0
n=0 (Exact)
x Long rectangular plate solution

FIG. 4

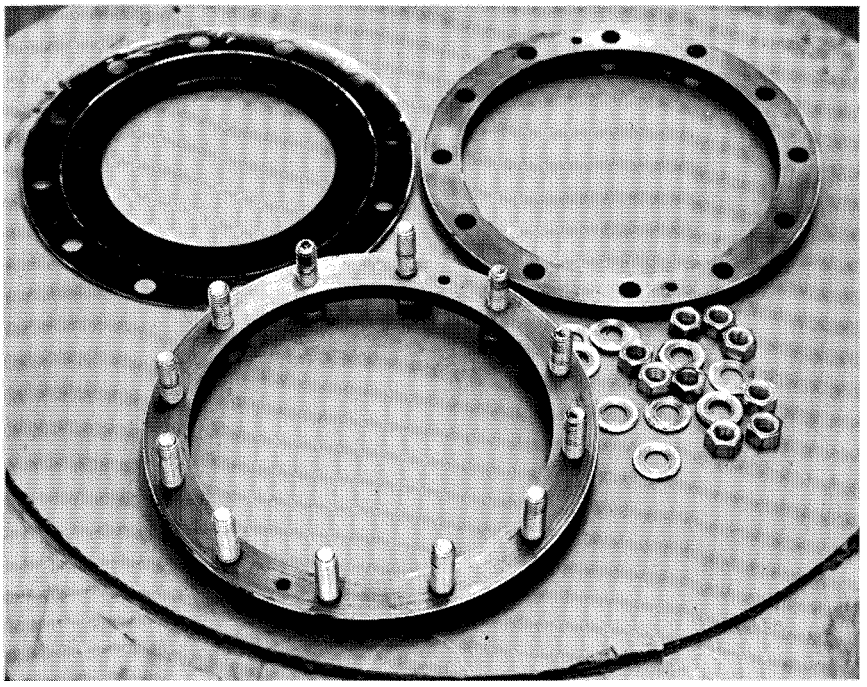

FIG. 5

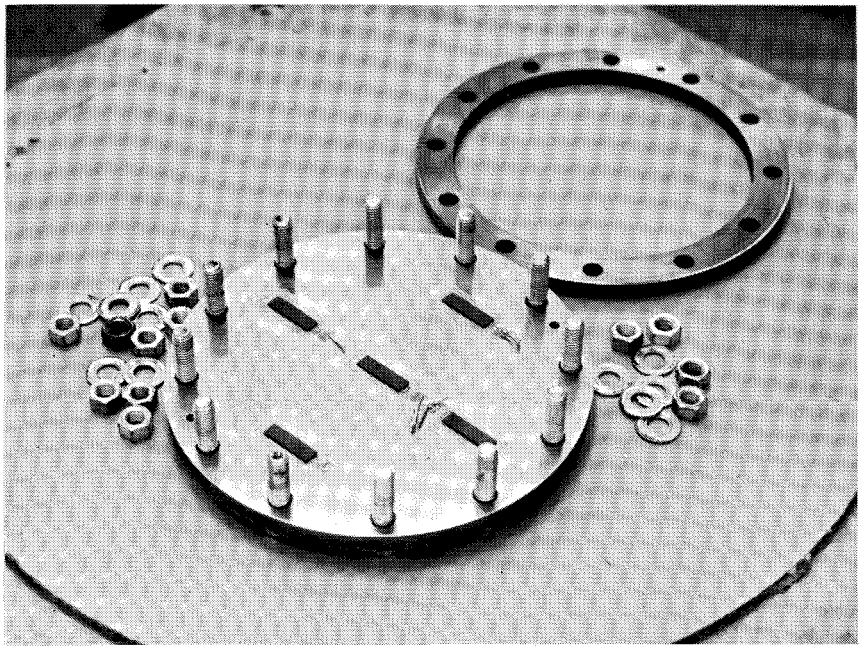

FIG. 6

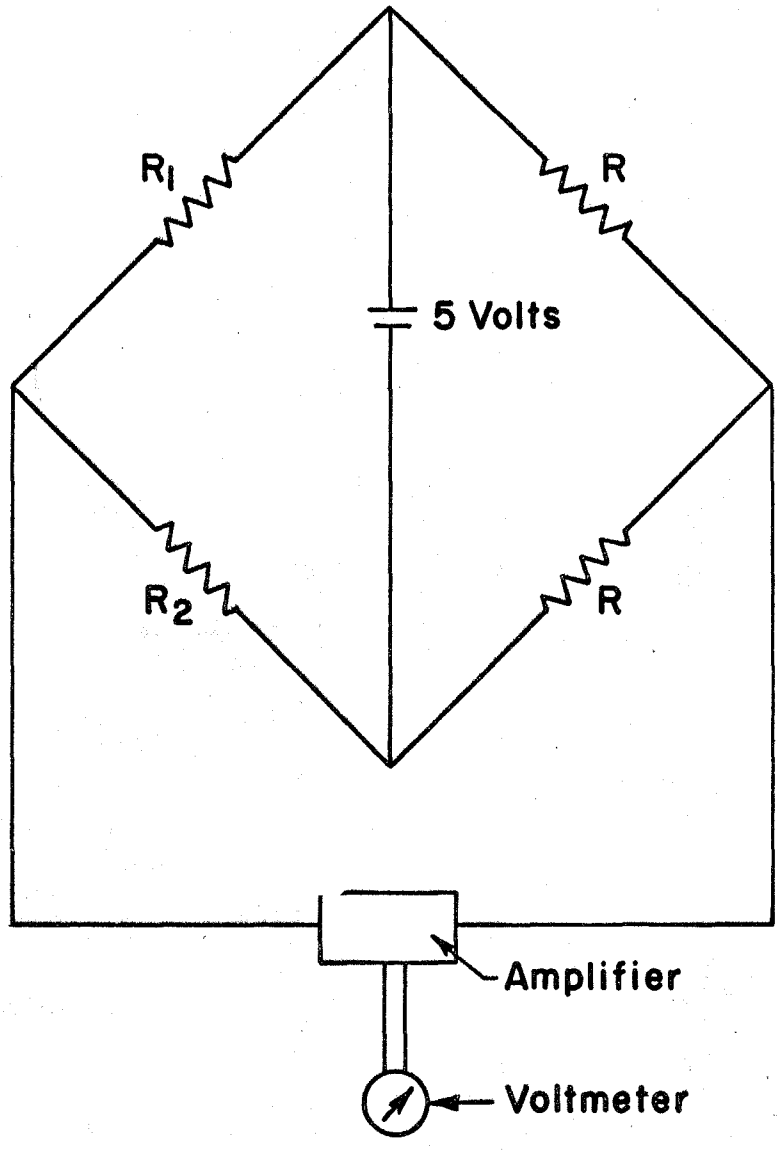

FIG. 7

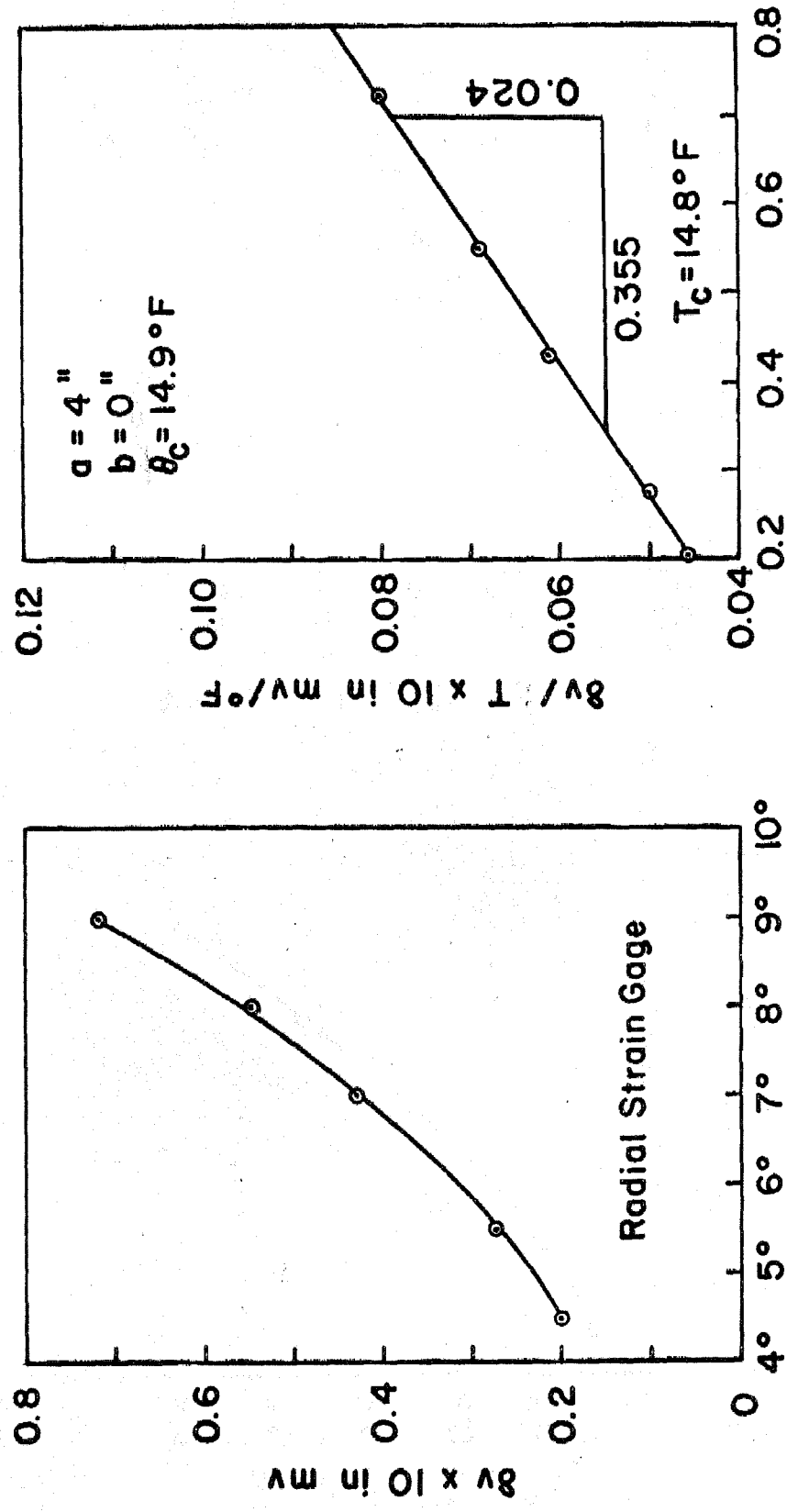
δv x 10 in mv
Southwell Plot
δv / T x 10 in mv/°F
a = 4"
b = 0"
θc = 14.9°F
0.355
0.024
Tc = 14.8°F
0.2
0.4
0.6
0.8
0.04
0.06
0.08
0.10
0.12
δv x 10 in mv
Radial Strain Gage
T in °F
0
0.2
0.4
0.6
0.8
4°
5°
6°
7°
8°
9°
10°

FIG. 8

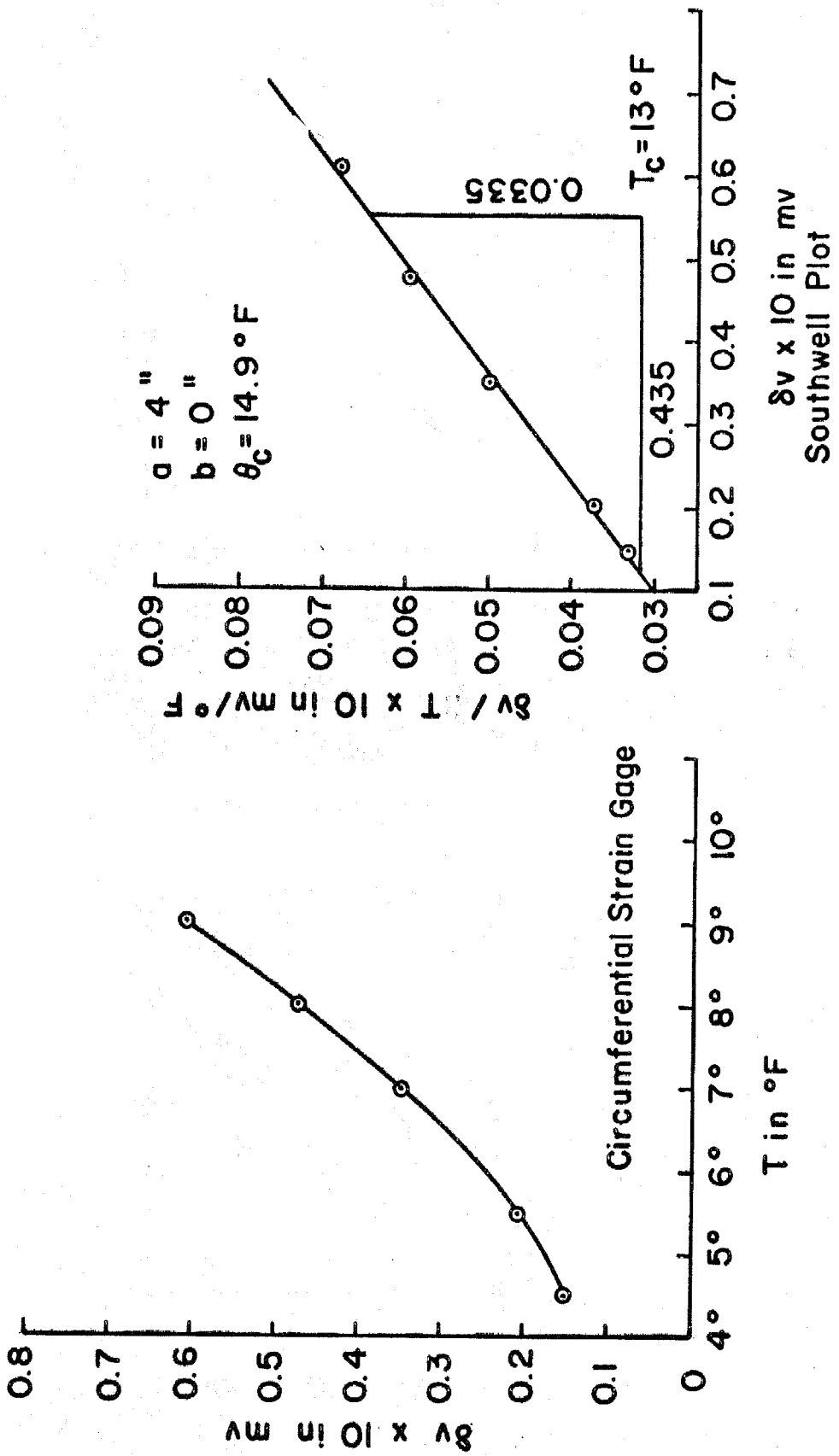
δv x 10 in mv
T in °F
Circumferential Strain Gage
0
0.1
0.2
0.3
0.4
0.5
0.6
0.7
0.8
4°
5°
6°
7°
8°
9°
10°
δv / T x 10 in mv/°F
0.03
0.04
0.05
0.06
0.07
0.08
0.09
0.1
0.2
0.3
0.4
0.5
0.6
0.7
0.435
0.0335
a = 4"
b = 0"
θc = 14.9°F
Tc = 13°F
δv x 10 in mv
Southwell Plot

FIG. 9

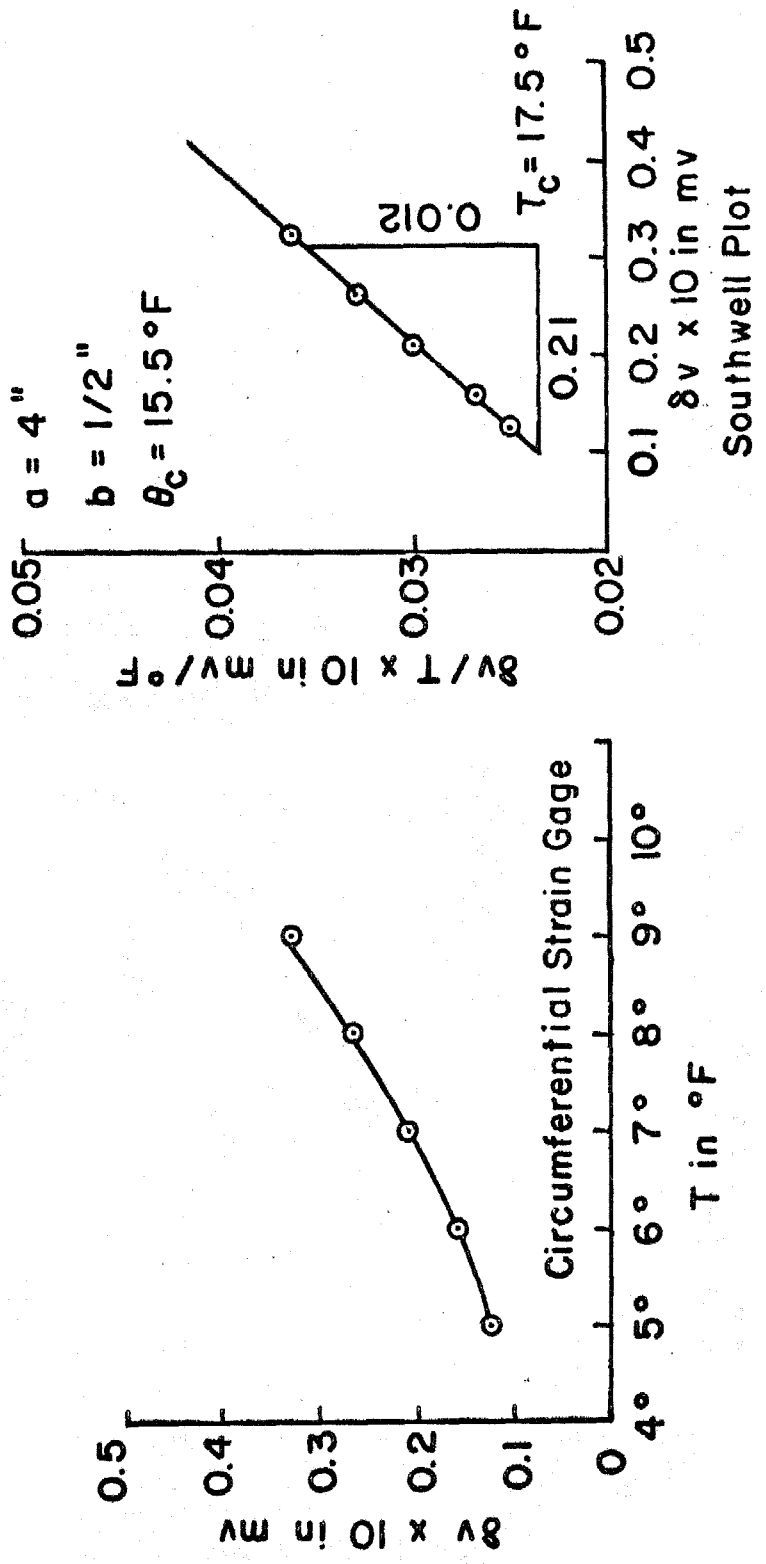
a = 4"
b = 1/2"
θ_c = 15.5°F
0.012
0.21
T_c = 17.5°F
δv/T x 10 in mv/°F
δv x 10 in mv
Circumferential Strain Gage
T in °F
δv x 10 in mv
Southwell Plot

FIG. 10

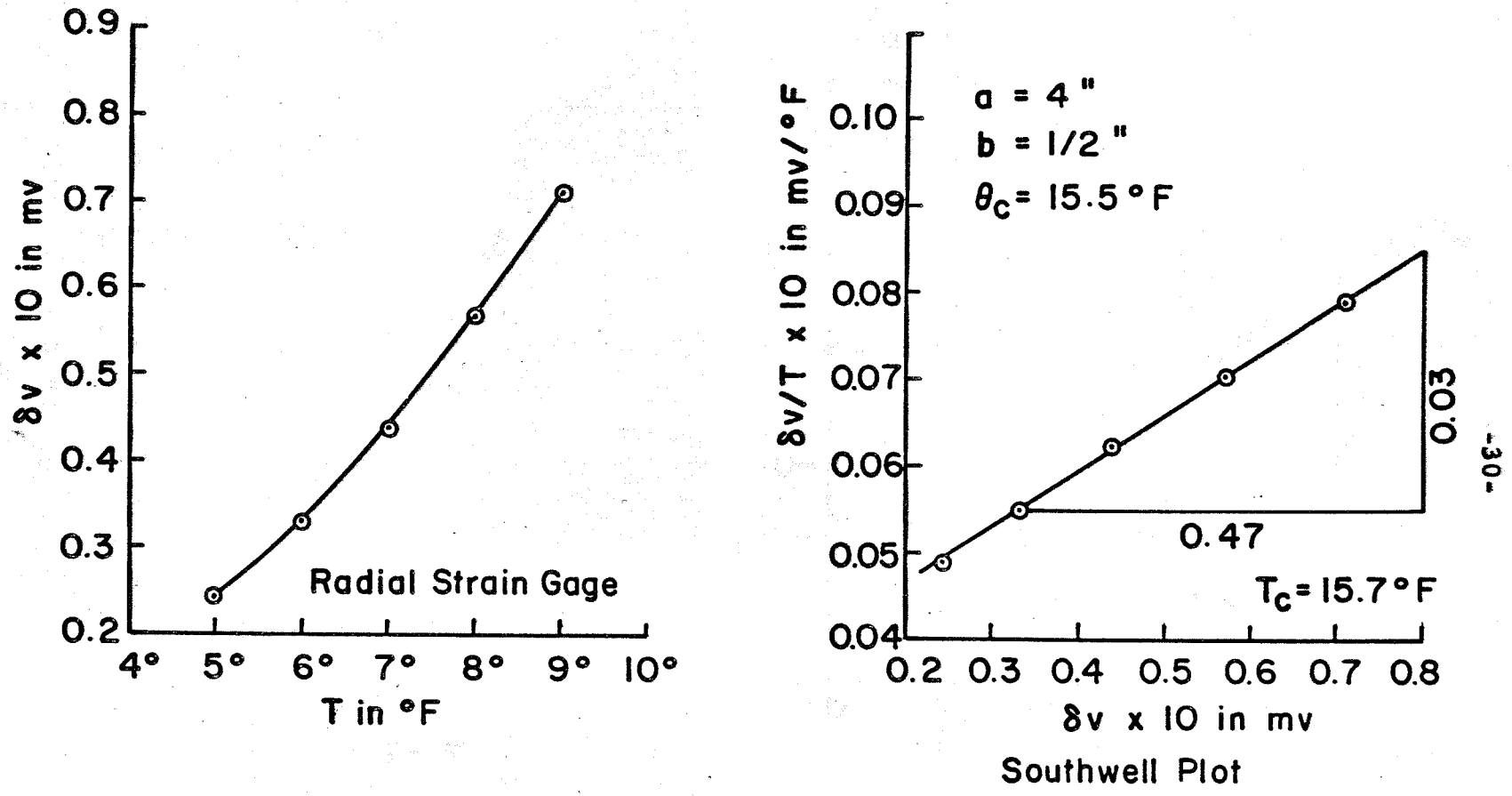
0.9
0.8
0.7
0.6
0.5
0.4
0.3
0.2
δv x 10 in mv
Radial Strain Gage
4° 5° 6° 7° 8° 9° 10°
T in °F
a = 4"
b = 1/2"
θc = 15.5 °F
0.10
0.09
0.08
0.07
0.06
0.05
0.04
δv/T x 10 in mv/°F
0.03
0.47
Tc = 15.7 °F
0.2 0.3 0.4 0.5 0.6 0.7 0.8
δv x 10 in mv
Southwell Plot

FIG. 11

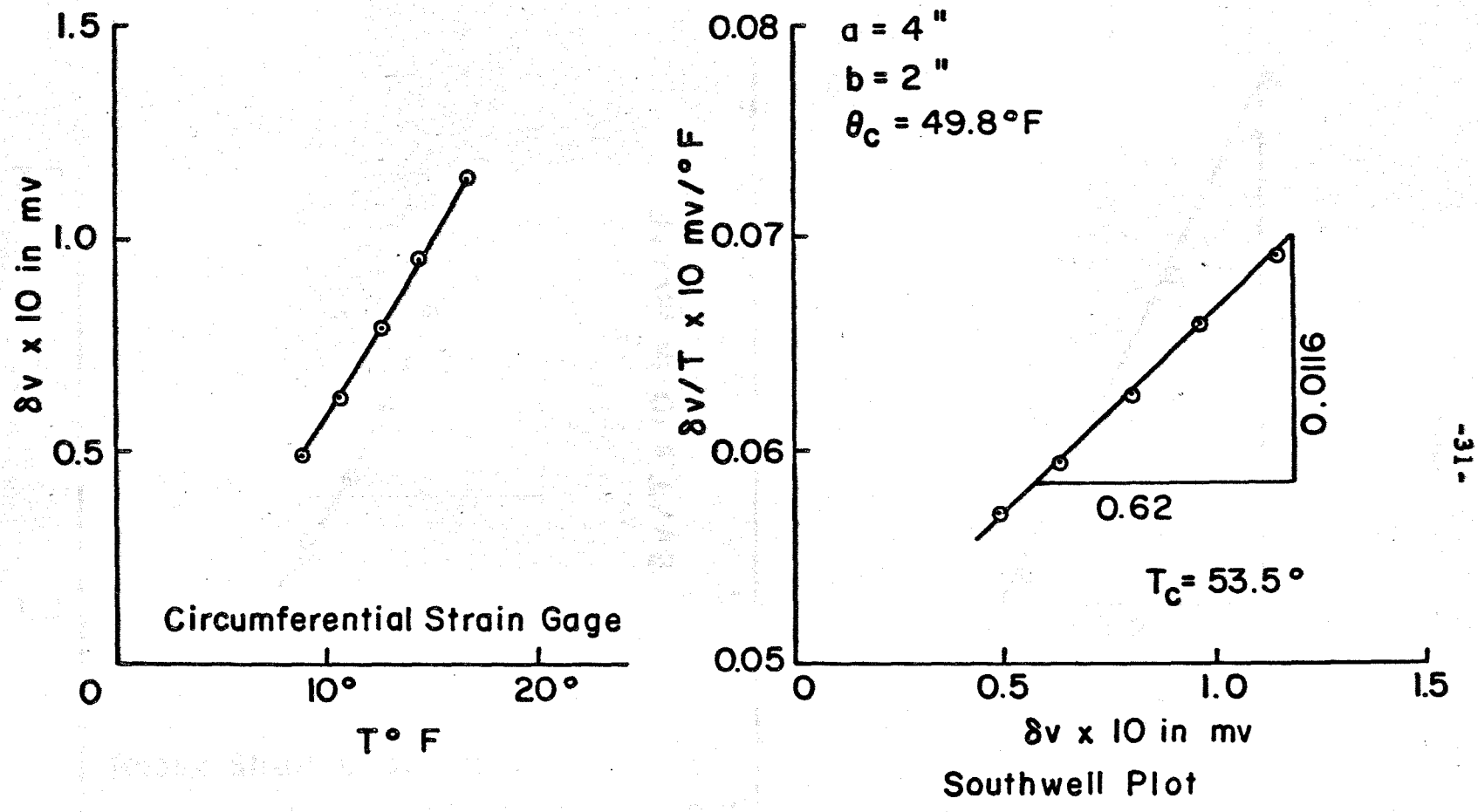
1.5
1.0
0.5
0
δv x 10 in mv
10°
20°
T° F
Circumferential Strain Gage
0.08
0.07
0.06
0.05
δv/T x 10 mv/°F
a = 4"
b = 2"
θc = 49.8°F
0.0116
0.62
Tc= 53.5°
0
0.5
1.0
1.5
δv x 10 in mv
Southwell Plot

FIG. 12

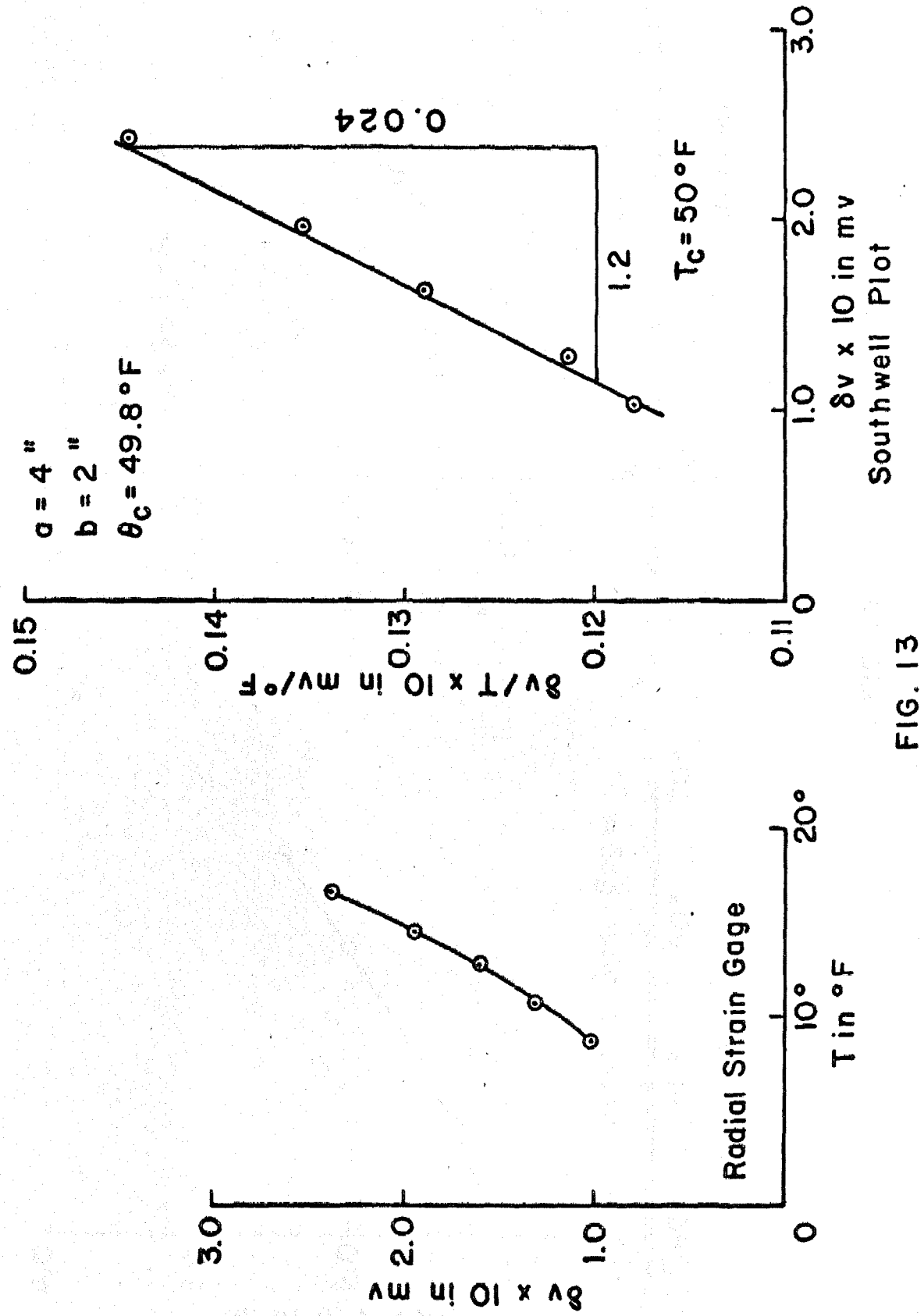
a = 4"
b = 2"
θ_c = 49.8°F
0.024
1.2
T_c = 50°F
δv/T x 10 in mv/°F
δv x 10 in mv
Southwell Plot
Radial Strain Gage
δv x 10 in mv
T in °F

FIG. 13

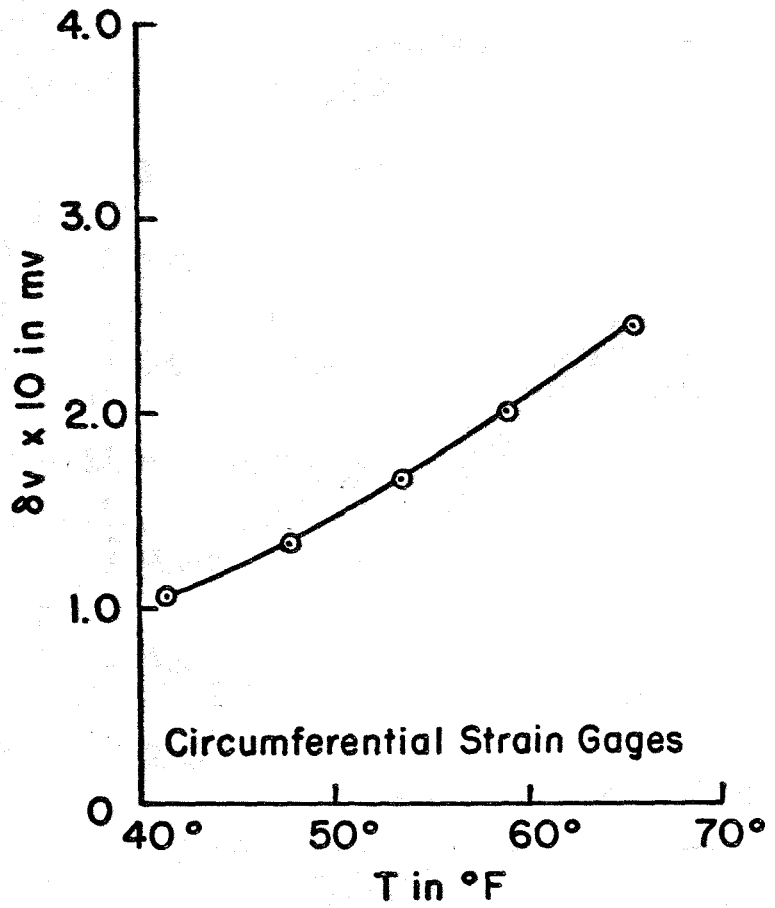
4.0
3.0
2.0
1.0
0
δv x 10 in mv
Circumferential Strain Gages
40°
50°
60°
70°
T in °F

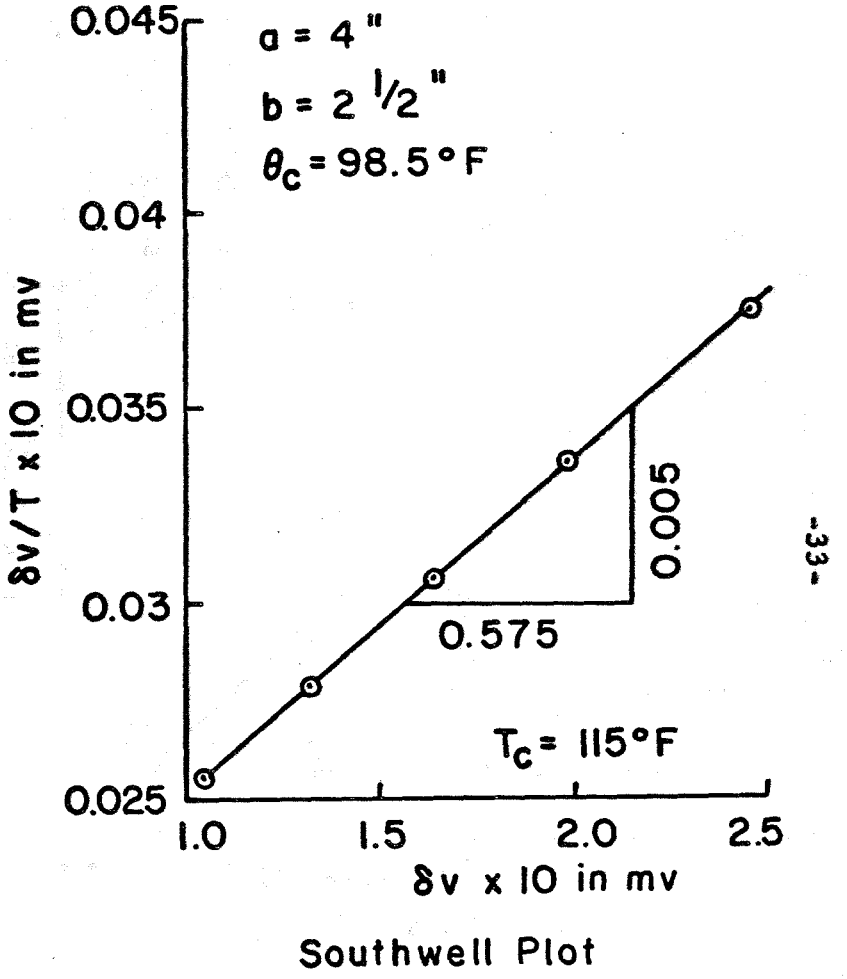
a = 4"
b = 2 1/2"
θc = 98.5°F
0.045
0.04
0.035
0.03
0.025
δv/T x 10 in mv
0.005
0.575
Tc = 115°F
1.0
1.5
2.0
2.5
δv x 10 in mv
Southwell Plot

FIG. 14

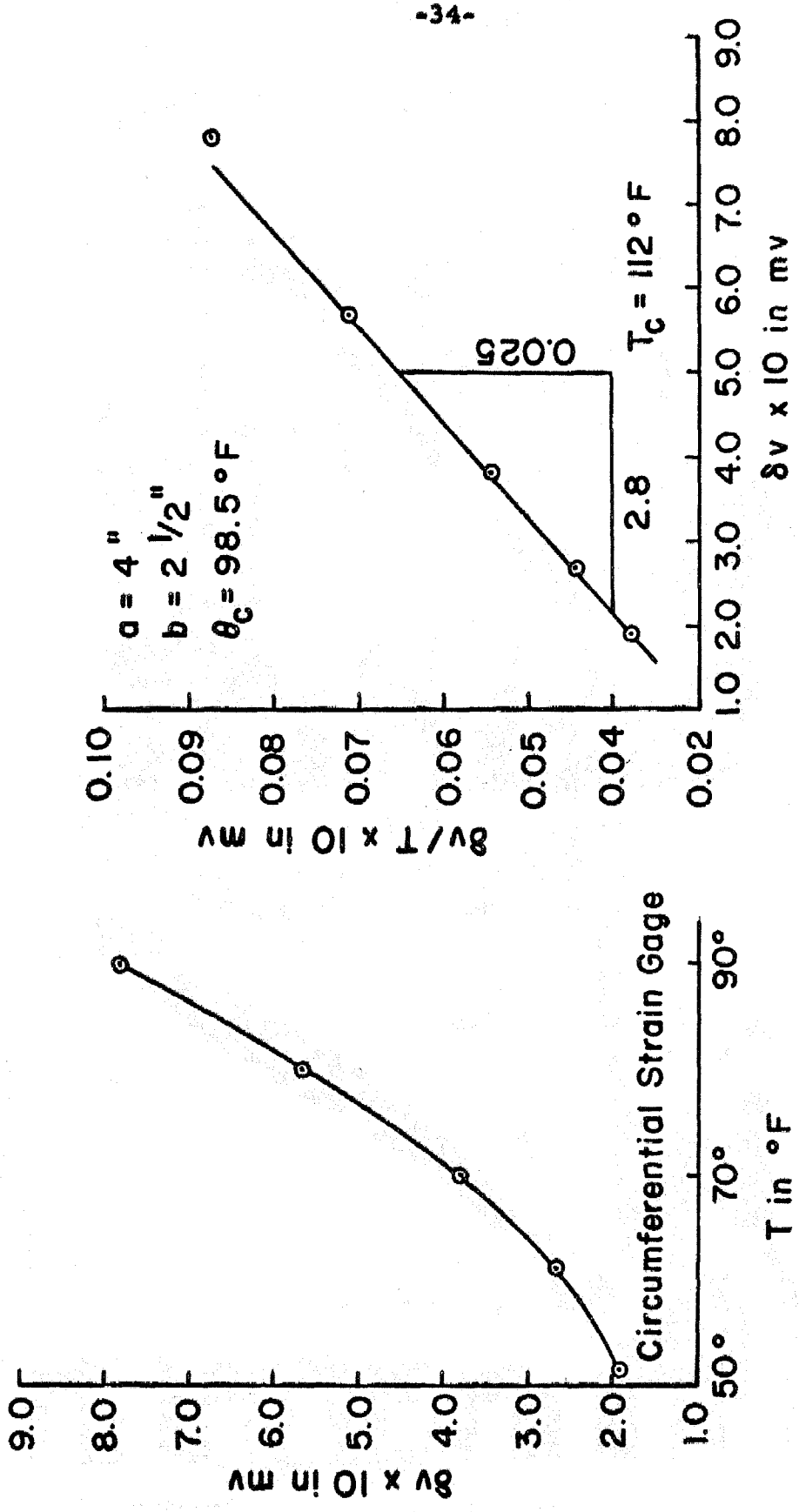
δv x 10 in mv
T in °F
Circumferential Strain Gage
50°
70°
90°
1.0
2.0
3.0
4.0
5.0
6.0
7.0
8.0
9.0
δv/T x 10 in mv
0.10
0.09
0.08
0.07
0.06
0.05
0.04
0.02
1.0 2.0 3.0 4.0 5.0 6.0 7.0 8.0 9.0
δv x 10 in mv
Southwell Plot
a = 4"
b = 2 1/2"
θc = 98.5 °F
2.8
0.025
Tc = 112 °F

FIG. 15

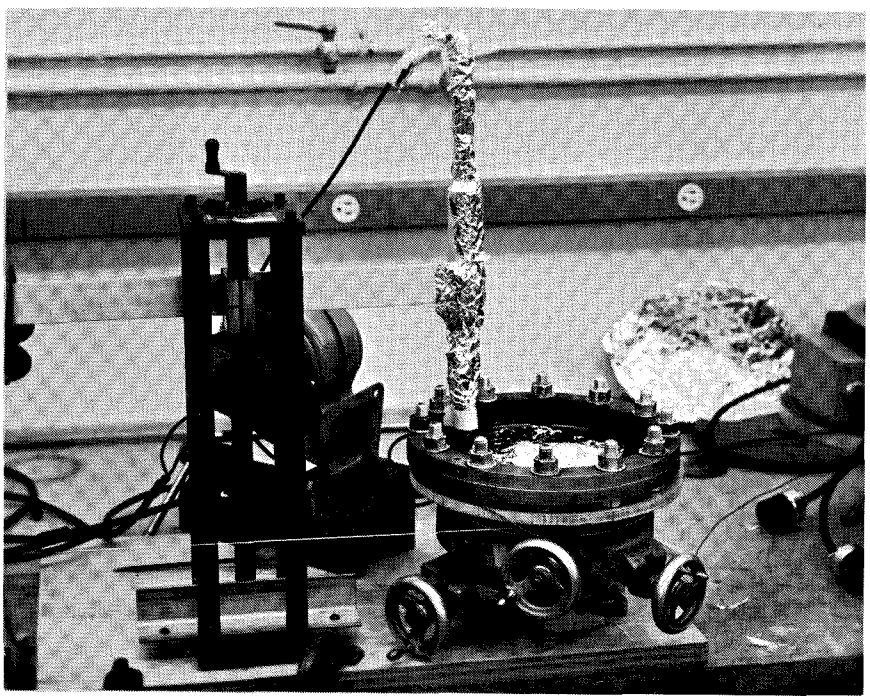

FIG. 16

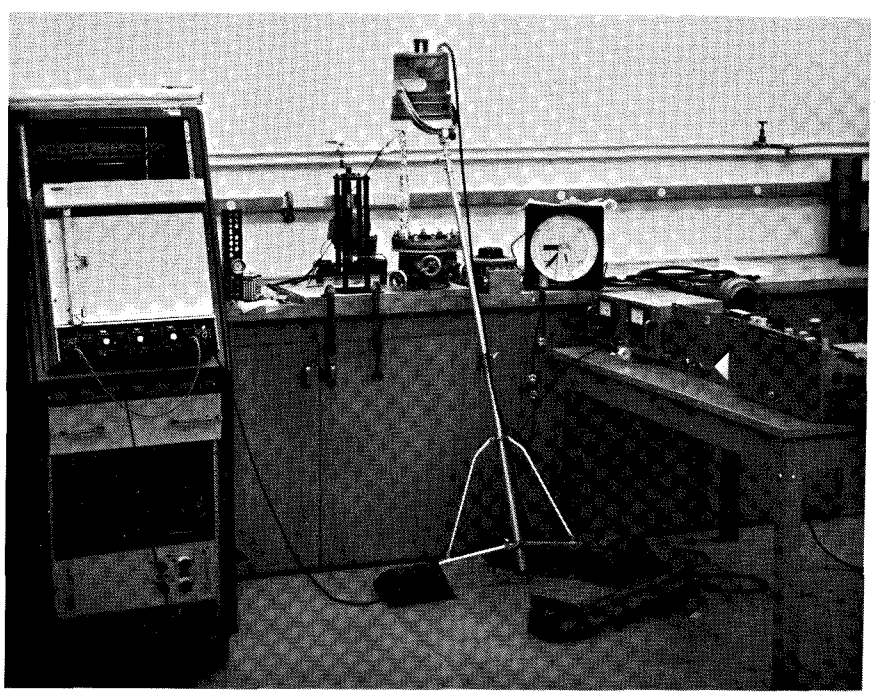

FIG. 17

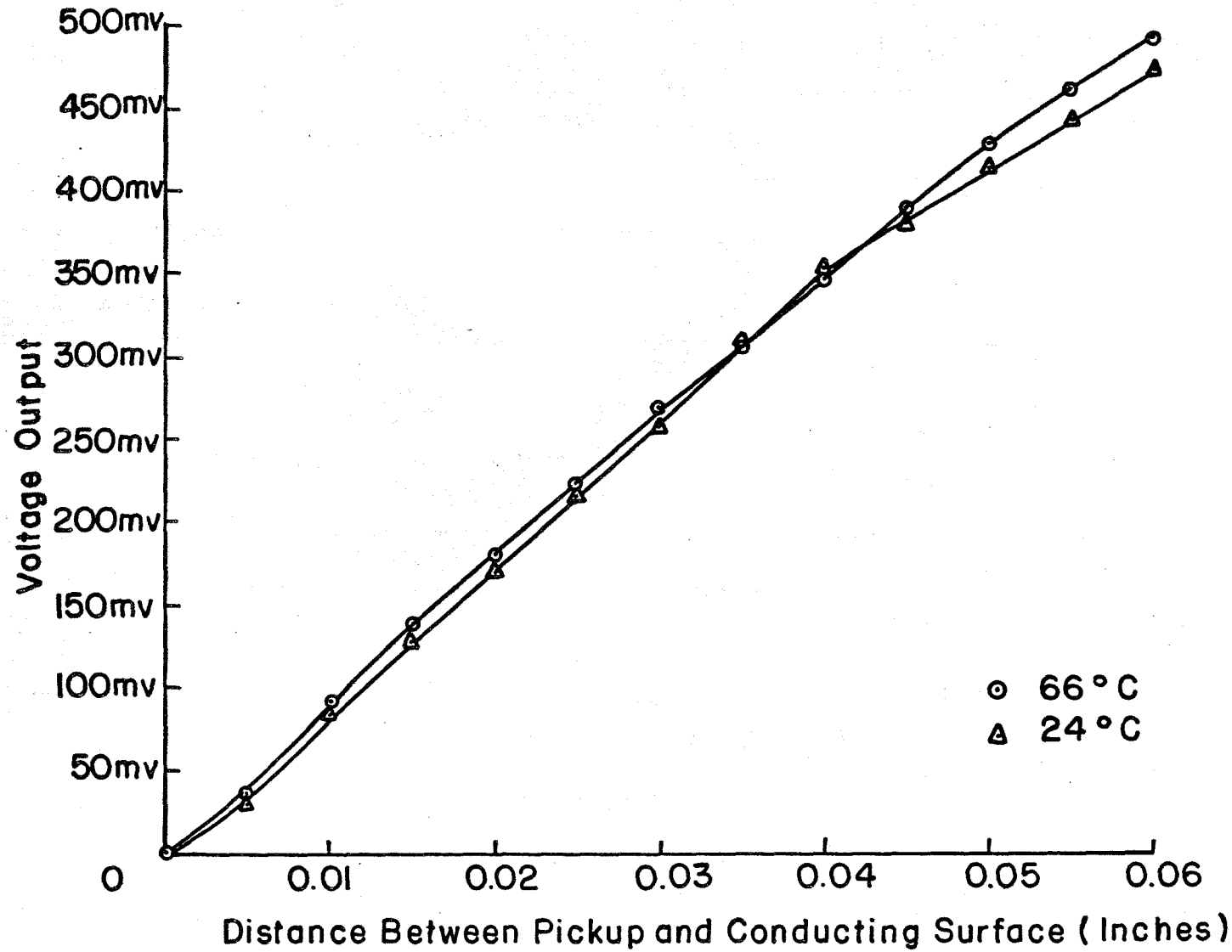

FIG. 18 CALIBRATION CURVE FOR PICKUP

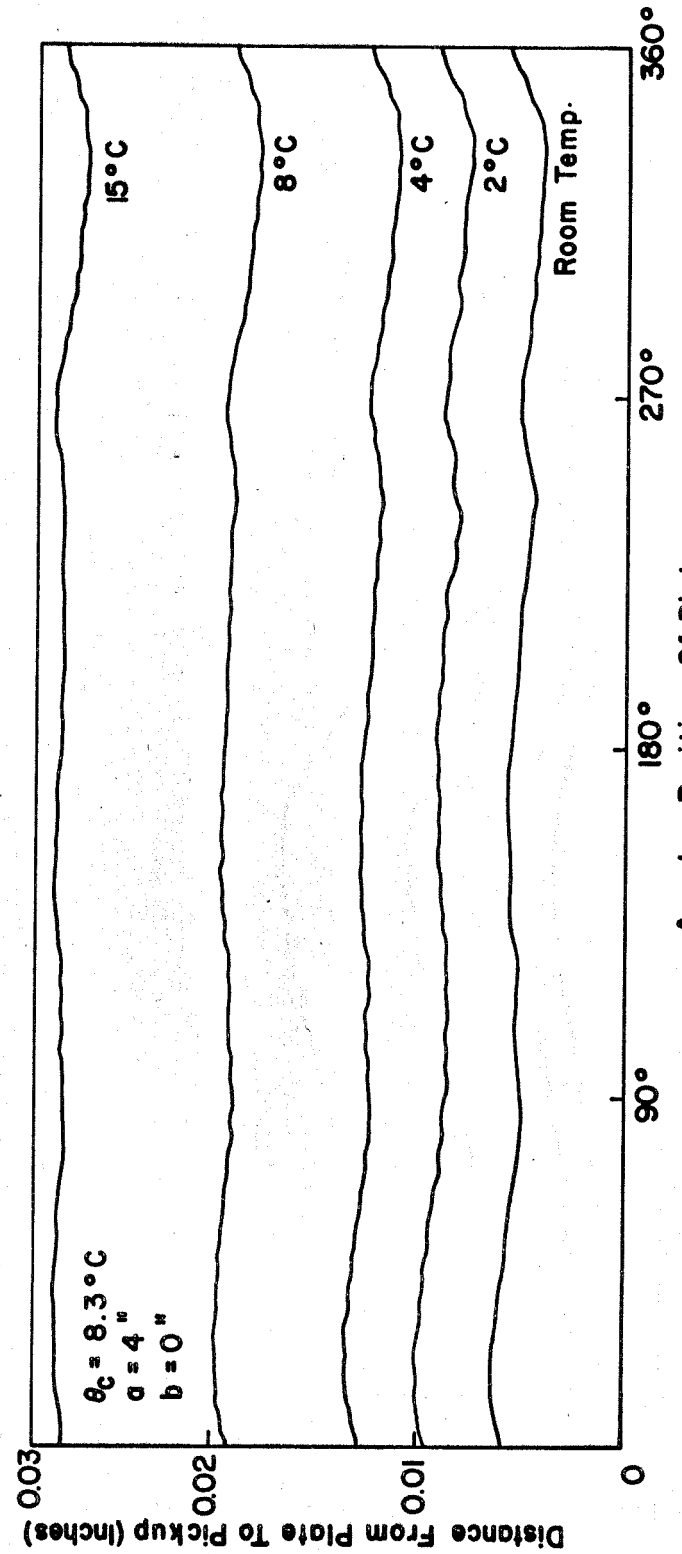
15°C
8°C
4°C
2°C
Room Temp.
θc = 8.3°C
a = 4"
b = 0"
0.03
0.02
0.01
0
90°
180°
270°
360°
Distance From Plate To Pickup (inches)
Angular Position Of Pickup

FIG. 19

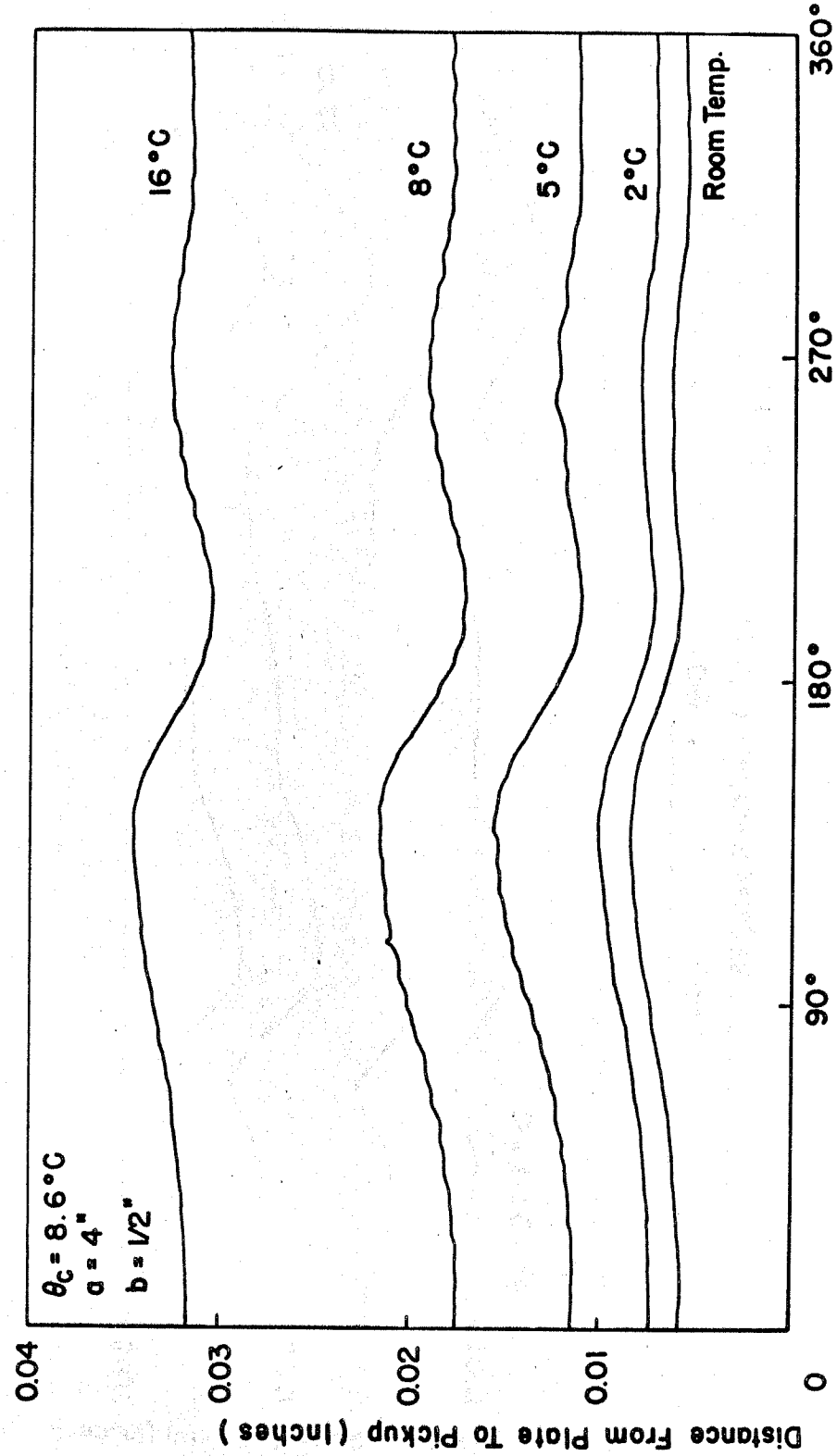
θ_c = 8.6°C
a = 4"
b = 1/2"
16°C
8°C
5°C
2°C
Room Temp.
0.04
0.03
0.02
0.01
0
90°
180°
270°
360°
Distance From Plate To Pickup (Inches)
Angular Position Of Pickup

FIG. 20

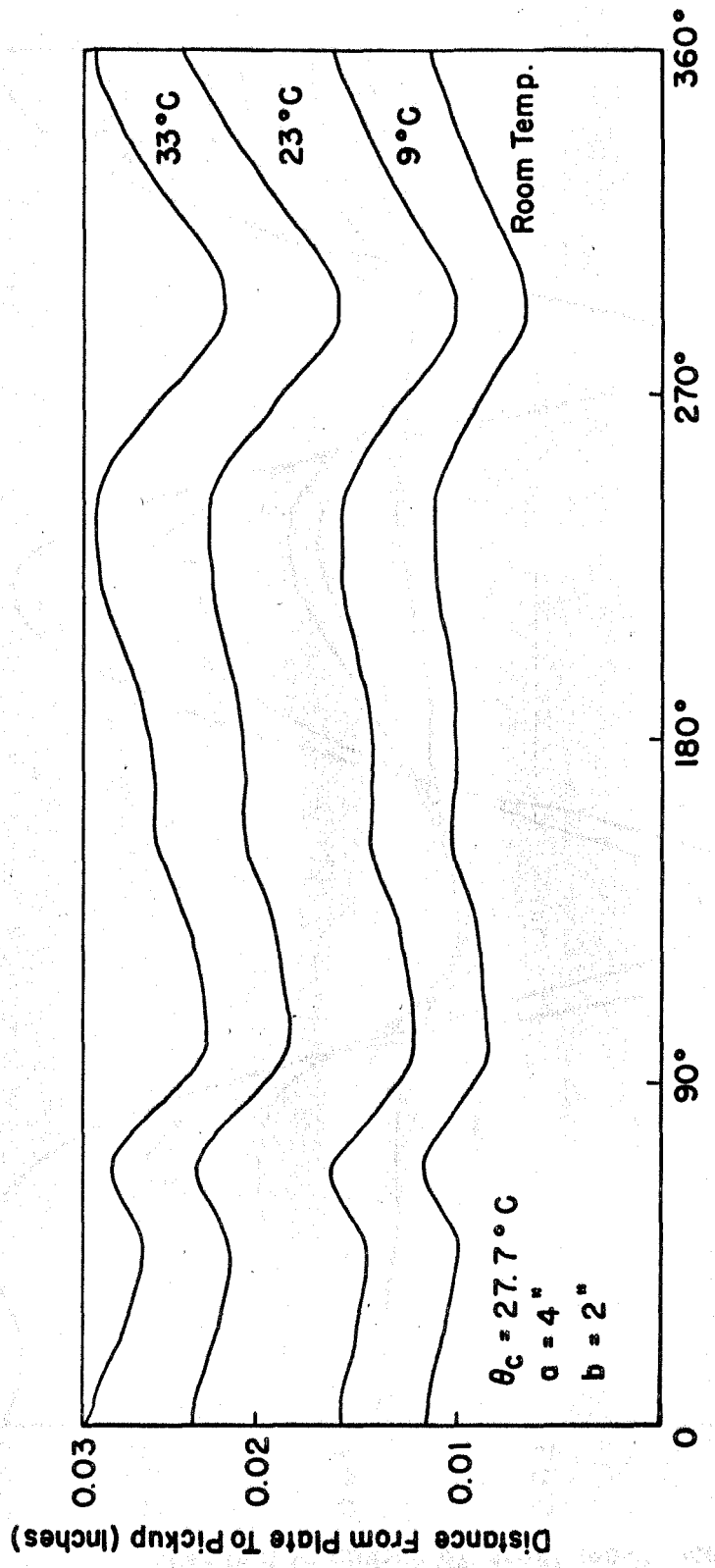
33°C
23°C
9°C
Room Temp.
θ_c = 27.7° C
a = 4"
b = 2"
0.03
0.02
0.01
0
90°
180°
270°
360°
Distance From Plate To Pickup (Inches)
Angular Position Of Pickup

FIG. 21

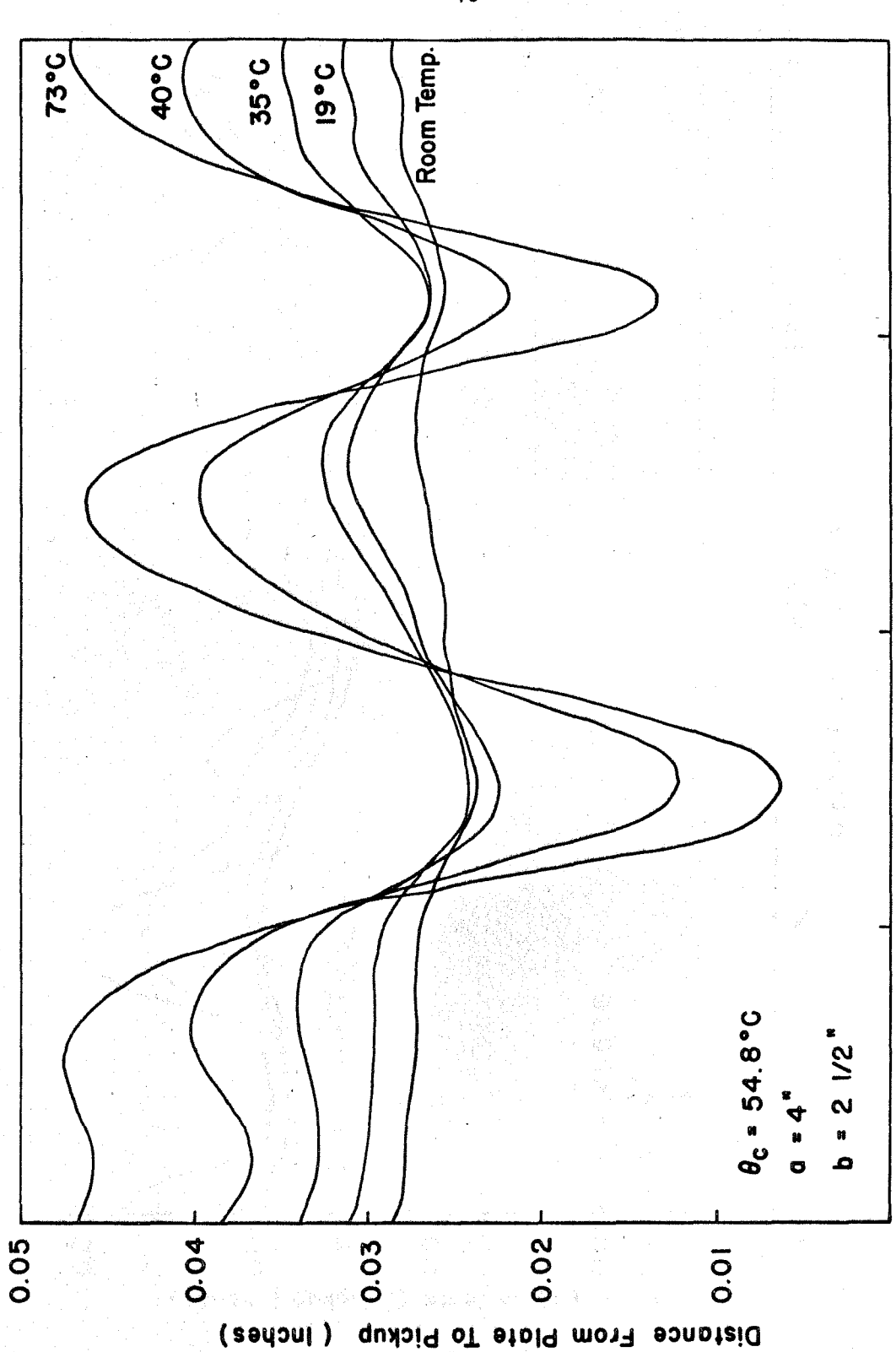
73°C
40°C
35°C
19°C
Room Temp.
θ_c = 54.8°C
a = 4"
b = 2 1/2"
0.05
0.04
0.03
0.02
0.01
Distance From Plate To Pickup (Inches)
0
90°
180°
270°
360°
Angular Position Of Pickup

FIG. 22

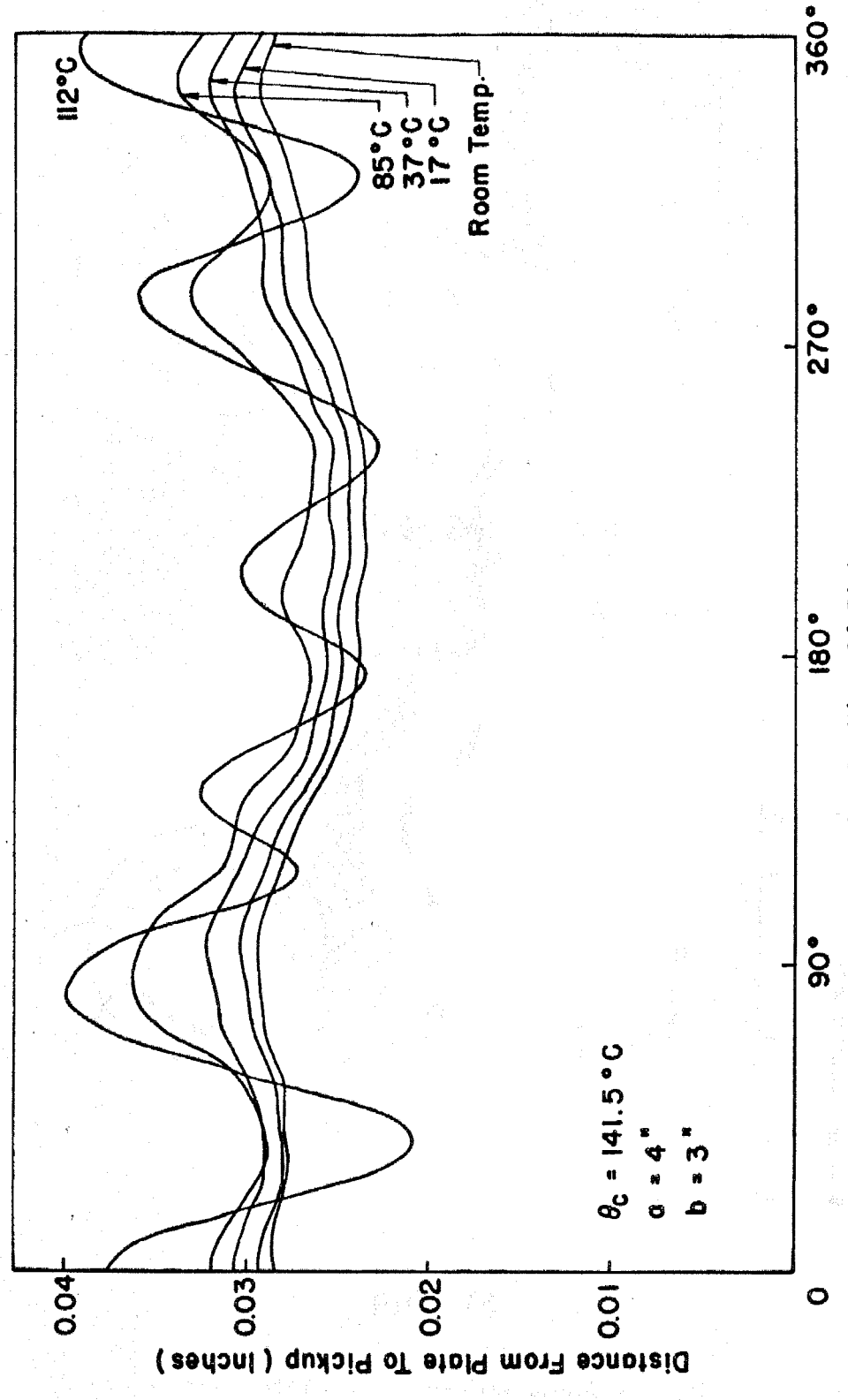
112°C
85°C
37°C
17°C
Room Temp.
θc = 141.5°C
a = 4"
b = 3"
0.04
0.03
0.02
0.01
Distance From Plate To Pickup (Inches)
0
90°
180°
270°
360°
Angular Position Of Pickup

FIG. 23

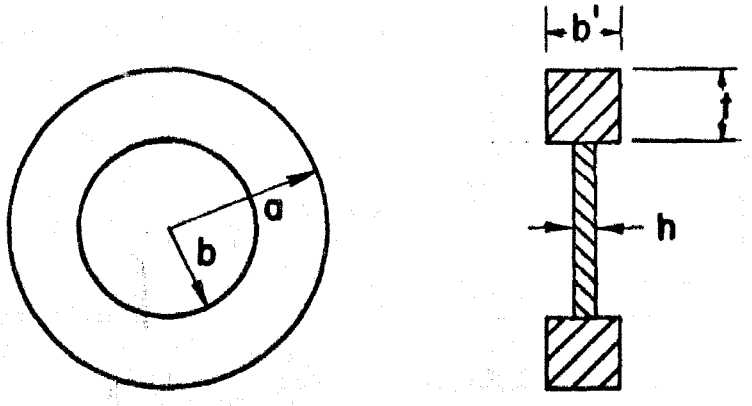

FIG. 24

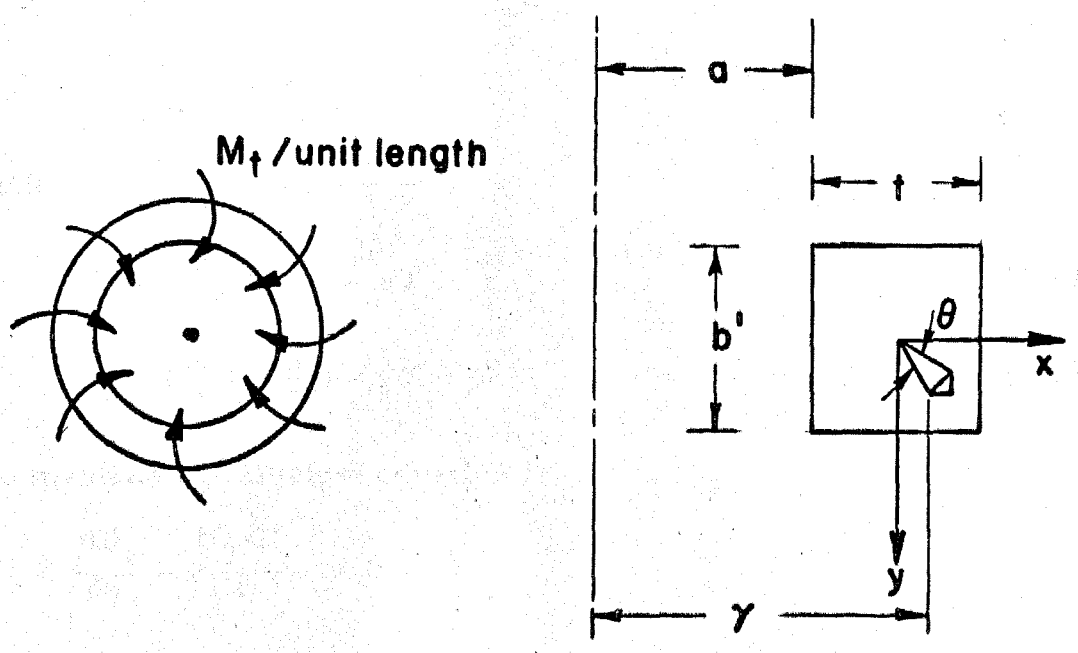

FIG. 25

APPENDIX A

Derivation of Buckling Temperature

$$e_r = \frac{1}{hE}(N_r - \nu N_\theta) + \alpha_A T$$

$$e_\theta = \frac{1}{hE}(N_\theta - \nu N_r) + \alpha_A T$$

Alternatively

$$N_r = \frac{hE}{1-\nu^2}(e_r + \nu e_\theta) - \frac{\alpha_A hET}{1-\nu}$$

$$N_\theta = \frac{hE}{1-\nu^2}(e_\theta + \nu e_r) - \frac{\alpha_A hET}{1-\nu}$$

Since displacements are radially symmetric

$$e_r = \frac{du}{dr}, \quad \text{and} \quad e_\theta = \frac{u}{r}$$

Letting $\beta = \frac{hE}{1-\nu^2}$ and $\gamma = \frac{\alpha hE}{1-\nu}$

$$N_r = \beta\left(\frac{du}{dr} + \nu\frac{u}{r}\right) - \gamma T \tag{32a}$$

$$N_\theta = \beta\left(\frac{u}{r} + \nu\frac{du}{dr}\right) - \gamma T \tag{32b}$$

The in-plane equilibrium equation is

$$\frac{dN_r}{dr} - \frac{N_\theta - N_r}{r} = 0$$

Substituting for N_r and N_θ in terms of u and T

$$\beta\frac{d^2u}{dr^2} + \frac{\nu\beta}{r}\frac{du}{dr} - \nu\beta\frac{u}{r^2} - \frac{\beta(1-\nu)\left(\frac{u}{r} - \frac{du}{dr}\right)}{r} = 0$$

or

$$\frac{d^2u}{dr^2} + \frac{1}{r}\frac{du}{dr} - \frac{u}{r^2} = 0$$

The solution is

$$u = Ar + B/r$$

Case I. Plate without hole

$$B = 0$$

and u at r = a is $\alpha_s Ta$, neglecting the elastic deformation of the rings.

$$\therefore \quad u = \alpha_s Tr$$

Putting the value of u in equation (32)

$$N_r = N_\theta = - \frac{hET}{1-\nu} (\alpha_A - \alpha_s) \tag{33}$$

From eq. (1)

$$N_{o_{cr}} = \frac{kEh^3}{12a^2(1-\nu^2)} = \frac{hE\theta_c}{1-\nu} (\alpha_A - \alpha_s)$$

$$\therefore \quad \theta_c = \frac{k}{12(1+\nu)} \frac{h^2}{a^2} \frac{1}{\alpha_A - \alpha_s} \tag{34}$$

Case II. Plate with hole

In this case the boundary conditions are

$$u = \alpha_s Ta \qquad \text{at} \quad r = a \tag{35a}$$

$$N_r = 0 \qquad \text{at} \quad r = b \tag{35b}$$

or $$Aa + \frac{B}{a} = \alpha_s Ta$$

$$\frac{hE}{1-\nu^2} \left(A - \frac{B}{b^2} + \nu A + \frac{\nu B}{b^2} \right) - \frac{\alpha_A hE}{1-\nu} T = 0$$

Solving for A and B and substituting for these in the solution for u

$$u = \frac{\alpha_s a^2(1-\nu)+\alpha_A b^2(1+\nu)}{a^2(1-\nu)+b^2(1+\nu)} Tr - \frac{(1+\nu)a^2b^2}{a^2(1-\nu)+b^2(1+\nu)} (\alpha_A-\alpha_s) \frac{T}{r}$$

Substituting this value of u in eq. (32)

$$N_r = - \frac{hETa^2}{a^2(1-\nu)+b^2(1+\nu)} (\alpha_A-\alpha_s) (1 - \frac{b^2}{r^2})$$

$$N_\theta = - \frac{hETa^2}{a^2(1-\nu)+b^2(1+\nu)} (\alpha_A-\alpha_s) (1 + \frac{b^2}{r^2})$$

From eq. (1)

$$N_{o_{cr}} = \frac{kEh^3}{12(1-\nu^2)a^2} = \frac{hE\theta_c a^2}{a^2(1-\nu)+b^2(1+\nu)} (\alpha_A-\alpha_s) (1 - \frac{b^2}{a^2})$$

$$\theta_c = \frac{k}{12(1-\nu^2)} \frac{a^2(1-\nu)+b^2(1+\nu)}{a^2-b^2} \frac{h^2}{a^2} \frac{1}{\alpha_A-\alpha_s} \qquad (36)$$

Effect of elasticity of ring on prebuckling stress distribution

In fig. 24, let p be the pressure on the plate applied by the ring. Then the pressure on the ring = $\frac{ph}{b'}$

∴ Radial displacement of ring

$$= \alpha_s Ta + \frac{ph}{b'} \frac{a^2}{E_s t}$$

Then the boundary condition (35a) should be replaced by

$$u = \alpha_s Ta + \frac{ph}{b'} \frac{a^2}{E_s t} \text{ at } r = a$$

or $$Aa + \frac{B}{a} = \alpha_s Ta + \frac{ph}{b'} \frac{a^2}{E_s t}$$

and the other equation is as before

$$\frac{hE}{1-\nu^2}\left(A - \frac{B}{b^2} + \nu A + \frac{\nu B}{b^2}\right) - \frac{\alpha_A hE}{1-\nu} T = 0$$

Solving

$$A = \frac{\alpha_s a^2(1-\nu)+\alpha_A b^2(1+\nu)}{a^2(1-\nu)+b^2(1+\nu)} T + \frac{ph\, a^3(1-\nu)}{b' E_s t \left\{a^2(1-\nu)+b^2(1+\nu)\right\}} \qquad (37a)$$

and

$$B = \frac{phb^2 a^3(1+\nu)}{b' E_s t\left\{a^2(1-\nu)+b^2(1+\nu)\right\}} - \frac{a^2 b^2(\alpha_A-\alpha_s)(1+\nu)T}{a^2(1-\nu)+b^2(1+\nu)} \qquad (37b)$$

Using the condition that $N_r = -ph$ at $r = a$

$$\frac{hE}{1-\nu^2}\left[A - \frac{B}{a^2} + \nu A + \frac{\nu B}{a^2}\right] - \frac{\alpha_A hE}{1-\nu} T = -ph$$

where A and B are given above.

Solving for p

$$p = \frac{\alpha_A-\alpha_s)\,(a^2-b^2)}{\frac{ha(a^2-b^2)}{b' t E_s} + \frac{a^2(1-\nu)+b^2(1+\nu)}{E}} T$$

This value of p substituted in eq. (37) gives the value of A and B in terms of T.

$$A = \frac{\alpha_s a^2(1-\nu)+\alpha_A b^2(1+\nu)}{a^2(1-\nu)+b^2(1+\nu)} T +$$

$$\frac{(1-\nu)T}{a^2(1-\nu)+b^2(1+\nu)} \quad \frac{(\alpha_A-\alpha_s)(a^2-b^2)ha^3}{ha(a^2-b^2)+b' t \frac{E_s}{E}\left\{a^2(1-\nu)+b^2(1+\nu)\right\}}$$

$$B = -\frac{(1+\nu)a^2b^2}{a^2(1-\nu)+b^2(1+\nu)}(\alpha_A-\alpha_s)T +$$

$$\frac{(\alpha_A-\alpha_s)(a^2-b^2)(1+\nu)ha^3b^2\,T}{\left[ha(a^2-b^2)+b't\frac{E_s}{E}\{a^2(1-\nu)+b^2(1+\nu)\}\right]\{a^2(1-\nu)+b^2(1+\nu)\}}$$

The second term in the expression for A and B give the correction due to elasticity of the ring. The magnitude of the correction has been calculated using the following data

$$\alpha_s = 6.7 \times 10^{-6} \text{ per } {}^\circ F,\ \alpha_A = 13.3 \times 10^{-6} \text{ per } {}^\circ F$$

$$\frac{E_s}{E} = 3 \quad b' = 1'' \quad t = 1'' ,\ \nu = .3$$

For $a = 4'', b = 0''$

$$A = 6.7 \times 10^{-6}T + .465 \times 10^{-6}\,T$$

% error in A for neglecting elasticity of ring

$$= \frac{.465}{7.165} \times 100 = 6.6$$

B = 0 for both cases.

For $a = 4'' \quad b = 2''$

$$A = 8.8 \times 10^{-6}\,T + .169 \times 10^{-6}\,T$$

% error in A for neglecting elasticity of ring

$$= \frac{.169}{8.969} \times 100 = 1.9$$

$$B = -33.3 \times 10^{-6}\,T + 1.25 \times 10^{-6}\,T$$

$\therefore$ % error in B for neglecting elasticity of ring

$$= \frac{1.25}{32.05} \times 100 = 3.9$$

The errors involved are seen to be small.

The effect of the twisting of the steel ring on the buckling load of the plate

Considering the ring acted on by the twisting moment M_t per unit length as shown in fig. 25, it can be shown (3) that the moment-rotation characteristic is given by

$$M_t = L\theta$$

where $L = \frac{E_s b'^3}{12a} \log (1 + t/a)$

Consider a solid circular plate loaded radially and clamped by elastic support with moment-rotation characteristic given by

$$M_t = L\theta$$

The equation of equilibrium is

$$rD\left(\frac{d^2}{dr^2} + \frac{1}{r}\frac{d}{dr}\right)\left(\frac{d^2w}{dr^2} + \frac{1}{r}\frac{dw}{dr}\right) + r N_o \frac{d^2w}{dr^2} + N_o \frac{dw}{dr} = 0$$

Let $\frac{N_o}{D} = \alpha^2$ and $\alpha r = u$, the above reduces to

$$\alpha^4 \left(\frac{d^2}{du^2} + \frac{1}{u}\frac{d}{du}\right)\left(\frac{d^2w}{du^2} + \frac{1}{u}\frac{dw}{du}\right) + \alpha^4 \frac{d^2w}{du^2} + \frac{\alpha^4}{u}\frac{dw}{du} = 0$$

or $$\frac{1}{u}\frac{d}{du}\left[u \frac{d}{du}\left\{\frac{1}{u}\frac{d}{du}\left(u \frac{dw}{du}\right)\right\}\right] + \frac{1}{u}\frac{d}{du}\left(u \frac{dw}{du}\right) = 0$$

The solution of this equation is

$$\phi = A_1 J_1(u) + B_1 Y_1(u) + C_1 S_{1,1}$$

where $\phi = \frac{dw}{du}$ and $S_{1,1}$ is the Lommel function.

Since ϕ is finite at u = 0, $B_1 = C_1 = 0$. The other boundary condition is

$$D\left(\frac{d^2w}{dr^2} + \frac{\nu}{a}\frac{dw}{dr}\right)\Bigg|_{r=a} = -L\frac{dw}{dr}\Bigg|_{r=a}$$

or $$\frac{d\phi}{du} + \left(\frac{\nu}{u} + \frac{L}{D\alpha}\right)\phi = 0 \quad \text{at } u = \alpha a$$

or $$J_o(\alpha a) - \frac{1}{\alpha a} J_1(\alpha a) + \left(\frac{\nu}{\alpha a} + \frac{L}{\alpha D}\right) J_1(\alpha a) = 0$$

or $$J_o(\alpha a) + \frac{1}{\alpha}\left(\frac{L}{D} - \frac{1-\alpha}{a}\right) J_1(/a) = 0$$

For the specimens used in the test

$$D \approx 50 \text{ lb in} \qquad L \approx 10^5 \text{ lbs}$$

$$\frac{L}{D} \approx 2000/\text{in} \qquad \nu = .3, \quad a = 4''$$

$$\therefore \quad J_o(4\alpha) + \frac{1}{\alpha}\left(2000 - \frac{.7}{4}\right) J_1(4\alpha) = 0$$

The solution is

$$4\alpha = 3.83$$

or $$N_{o_{cr}} = .9786D$$

For a perfectly clamped plate

$$N_{o_{cr}} = .9788D$$

Thus for the specimens used the assumption of perfectly clamped edge condition is justified and can reasonably be extended to plates with holes.

APPENDIX B

The pair of radial strain gauges used in test series A measures the difference in the radial strains and a pair of circumferential strain gauges measures the difference in the circumferential strains between the top and the bottom surfaces of the plate.

$$\sigma_r(\text{top}) = \frac{E\frac{t}{2}}{1-\nu^2}\left\{\frac{d^2w}{dr^2} + \frac{\nu}{r}\frac{dw}{dr}\right\}$$

$$\sigma_\theta(\text{top}) = \frac{E\frac{t}{2}}{1-\nu^2}\left\{\frac{1}{r}\frac{dw}{dr} + \nu\frac{d^2w}{dr^2}\right\}$$

$$\therefore \quad e_r(\text{top}) = \frac{\sigma_r(\text{top})}{E} - \nu\frac{\sigma_\theta(\text{top})}{E}$$

$$= \frac{t}{2}\frac{d^2w}{dr^2}$$

$$e_\theta(\text{top}) = \frac{t}{2}\frac{1}{r}\frac{dw}{dr}$$

$$\therefore \quad e_r(\text{top}) - \epsilon_r(\text{bottom}) = t\frac{d^2w}{dr^2} \tag{38a}$$

$$e_\theta(\text{top}) - \epsilon_\theta(\text{bottom}) = \frac{t}{r}\frac{dw}{dr} \tag{38b}$$

Thus the pair of radial strain gauges measure the radial curvature of the plate and the pair of the circumferential gauges measure the circumferential curvature of the plate.

Imperfect plate

Consider a solid circular plate with radially symmetric initial imperfection $w_o(r)$. The equation of equilibrium is (for small w and w_o)

$$\nabla^4 w + \frac{N_o}{D}\nabla^2(w + w_o) = 0$$

Since the deflections are radially symmetric

$$\frac{1}{r}\frac{d}{dr}\left[r\frac{d}{dr}\left\{\frac{1}{r}\frac{d}{dr}\left(r\frac{dw}{dr}\right)\right\}\right] + \frac{N_o}{D}\frac{1}{r}\frac{d}{dr}\left(r\frac{d(w+w_o)}{dr}\right)$$

$$\therefore \quad r\frac{d}{dr}\left\{\frac{1}{r}\frac{d}{dr}\left(r\frac{dw}{dr}\right)\right\} + \frac{N_o}{D}r\frac{d(w+w_o)}{dr} = C_1$$

Since there is no lateral load $C_1 = 0$.

Letting $\frac{dw}{dr} = \phi$ and substituting $\alpha r = u$, where $\alpha^2 = \frac{N_o}{D}$

$$u^2\frac{d^2\phi}{du^2} + u\frac{d\phi}{du} + (u^2-1)\phi = -\alpha u^2\frac{dw_o}{du}$$

Let $J_1(\alpha a) = 0$ have roots $\alpha_1, \alpha_2, \ldots\ldots$

Let $$\frac{1}{\alpha}\phi_o = \frac{dw_o}{du} = \sum_{n=1}^{\infty} a_n J_1\left(\frac{\alpha_n}{\alpha}u\right) = \sum_{n=1}^{\infty}\frac{1}{\alpha}b_n J_1(\alpha_n r)$$

where $\phi_o = \frac{dw_o}{dr}$

The equation reduces to

$$u^2\frac{d^2\phi}{du^2} + u\frac{d\phi}{dn} + (u^2-1)\phi = -\alpha u^2\sum_{n=1}^{\infty}a_n J_1\left(\frac{\alpha_n}{\alpha}u\right)$$

with boundary conditions $\phi = 0$ at $u = 0$ and $\phi = 0$ at $u = \alpha a$.

The Green's function for this operator is

$$G(u,\xi) = \begin{cases} \frac{\pi\xi}{2}\left[Y_1(\xi) - \frac{J_1(\xi)Y_1(\alpha a)}{J_1(\alpha a)}\right]J_1(u) \text{ for } 0 \leq u \leq \xi \\ \\ \frac{\pi\xi}{2}\left[J_1(\xi)Y_1(u) - \frac{J_1(\xi)Y_1(\alpha a)}{J_1(\alpha a)}J_1(a)\right] \text{ for } \xi \leq u \leq \alpha a \end{cases}$$

Using the Green's function the solution of the above differential equation can be written as

$$\phi = \sum_{n=1}^{\infty} \frac{\pi a a_n}{2\left\{\left(\frac{a_n}{a}\right)^2 - 1\right\}} u J_1\left(\frac{a_n}{a} u\right) \left\{Y_1(u)J_2(u) - Y_2(u)J_1(u)\right\}$$

or $$\phi = \sum_{n=1}^{\infty} \frac{\pi b_n}{2\left\{\left(\frac{a_n}{a}\right)^2 - 1\right\}} ar J_1(a_n r) \left\{Y_1(ar)J_2(ar) - Y_2(ar)J_1(ar)\right\} \tag{39}$$

For small load N_o, this can be written as

$$\phi = \sum_{n=1}^{\infty} \frac{b_n J_1(a_n r)}{\left\{\left(\frac{a_n}{a}\right)^2 - 1\right\}} \left[1 - \frac{1}{192}\left(\frac{N_o}{D}\right)^2 r^4 + O\left\{\left(\sqrt{\frac{N_o}{D}}\, r\right)^6\right\}\right]$$

Taking only the first two terms of the series

$$\phi = \frac{b_1\left(1 - \frac{1}{192}\left(\frac{N_o}{D}\right)^2 r^4\right)}{\left(\frac{a_1}{a}\right)^2 - 1} J_1(a_1 r) + \frac{b_2\left(1 - \frac{1}{192}\left(\frac{N_o}{D}\right)^2 r^4\right)}{\left(\frac{a_2}{a}\right)^2 - 1} J_1(a_2 r)$$

$$= \frac{b_1\left\{1 - .071\left(\frac{N_o}{N_{o_{cr}}}\right)^2 \left(\frac{2r}{a}\right)^4\right\}}{\frac{N_{o_{cr}}}{N_o} - 1} J_1(a_1 r) + \frac{b_2\left\{1 - .071\left(\frac{N_o}{N_{o_{cr}}}\right)^2 \left(\frac{2r}{a}\right)^4\right\}}{3.4\,\frac{N_{o_{cr}}}{N_o} - 1} J_1(a_2 r)$$

(using $a_1 = \frac{3.8}{a}$ and $a_2 = \frac{7.01}{a}$)

Coefficients of b_1 and b_2 together with the first order correction are tabulated on the following page for $r = a/2$.

$\frac{N_o}{N_{o_{c_r}}}$	Coefficient of b_1		Coefficient of b_2	
	Oth order	Correction	Oth order	Correction
.1	.0644	-.0000	.0047	-.0000
.2	.1450	-.0006	.0082	.0000
.3	.2500	-.0017	.0136	-.0001
.4	.3800	-.0046	.0188	-.0002
.5	.5800	-.0104	.0242	-.0004
.6	.8700	-.0220	.0300	-.0007
.7	1.3334	-.0470	.0364	-.0013
.8	2.32	-.1055	.0431	-.0020

Thus for $\frac{N_o}{N_{o_{cr}}} \ll 1.0$, the relation

$$\phi = \frac{dw}{dr} = \frac{b_1}{\frac{N_{o_{cr}}}{N_o} - 1} J_1(a_1 r) \tag{40}$$

is quite accurate.

Differentiating eq. (39) it can be shown that

$$\frac{d^2w}{dr^2} = \sum_{n=1}^{\infty} \frac{\pi b_n a}{2\left[\left(\frac{a_n}{a}\right)^2 - 1\right]} \left[a_n r J_1'(a_n r)\left\{Y_1(ar)J_2(ar) - Y_2(ar)J_1(ar)\right\}\right]$$

where $J_1'(a_n r) = \frac{dJ_1(a_n r)}{dr}$

defining

$$\chi_o = \frac{d^2 w_o}{dr^2} = \sum_{n=1}^{\infty} a_n b_n J_1'(a_n r) = \sum_{n=1}^{\infty} C_n J_1'(a_n r)$$

the above reduces to

$$\frac{d^2w}{dr^2} = \sum_{n=1}^{\infty} \frac{\pi C_n}{\frac{a}{2}\left\{\left(\frac{a_n}{a}\right)^2 - 1\right\}} \, ar \, J_1'(a_n r) \left\{Y_1(ar)J_2(ar) - Y_2(ar)J_1(ar)\right\}$$

and as before for small loading

$$\frac{d^2w}{dr^2} = \sum_{n=1}^{\infty} \frac{C_n J_1'(a_n r)}{\left\{\left(\frac{a_n}{a}\right)^2 - 1\right\}} \left[1 - \frac{1}{192}\left(\frac{N_o}{D}\right)^2 r^4 + O\left(\sqrt{\frac{N_o}{D}}\, r\right)^6\right]$$

and also for $\frac{N_o}{N_{o_{cr}}} << 1.0$

$$\frac{d^2w}{dr^2} = \frac{C_1}{\frac{N_{o_{cr}}}{N_o} - 1} J_1'(a_n r) \tag{41}$$

is quite accurate.

Thus from eqs. (38a), (38b), and (40) and (41) we conclude that a Southwell type plot may be used with the test data to find the buckling load.